ERCB/AGS Open File Report 2008-10

ERCB

Geochemical and Sedimentological Investigation of the Banff and Exshaw Formations for Shale Gas Potential: Initial Results

Energy Resources Conservation Board

AGS
Alberta Geological Survey

ERCB/AGS Open File Report 2008-10

Geochemical and Sedimentological Investigation of the Banff and Exshaw Formations for Shale Gas Potential: Initial Results

C.D. Rokosh, J.G. Pawlowicz, H. Berhane, S.D.A. Anderson and A.P. Beaton

Energy Resources Conservation Board
Alberta Geological Survey

March 2009

ISBN 978-0-7785-6971-8

Rokosh, C.D., Pawlowicz, J.G., Berhane, H., Anderson, S.D.A. and Beaton, A.P. (2008): Geochemical and sedimentological investigation of the Banff and Exshaw formations for shale gas potential: initial results; Energy Resources Conservation Board, ERCB/AGS Open File Report 2008-10, 46 p.

Published March 2009 by:
Energy Resources Conservation Board
Alberta Geological Survey
4th Floor, Twin Atria Building
4999 – 98th Avenue
Edmonton, Alberta
T6B 2X3
Canada
Tel: 780.422.3767
Fax: 780.422.1918
E-mail: AGS-Info@ercb.ca
Website: www.ags.gov.ab.ca

Contents

Acknowledgments vi
Abstract vii
1 Introduction 1
2 Stratigraphy of the Banff and Exshaw Formations 1
2.1 Mississippian Banff and Exshaw Formations Stratigraphy 1
2.1.1 Banff Formation Stratigraphic Cross-Section B8 (64-10W5 to 54-25W5) 5
2.1.2 Banff Formation Stratigraphic Cross-Section B14 (1-21W4 to 32-14W4) 5
3 Methodology of Sampling and Testing 6
3.1 Rock Eval™ 6 and Total Organic Carbon (TOC) 8
3.2 Organic Petrology 9
3.3 Isotherm (Adsorption) Analysis 9
3.4 X-Ray Powder Diffraction (XRD) and Whole-Rock and Clay Mineralogy 9
3.5 Petrographic Analysis (Thin Section) 9
3.6 Permeametry 10
3.7 Mercury Porosimetry and Helium Pycnometry 10
3.8 Scanning Electron Microscope (SEM) and Environmental Scanning Electron Microscopy (ESEM) 10
4 Shale Gas Data Analysis 10
4.1 Geochemistry Results 11
4.1.1 Organic Geochemistry as an Indicator of Shale Gas Potential 11
4.1.2 Results of the Analysis 12
4.1.2.1 Banff Formation 12
4.1.2.2 Exshaw Formation 12
4.1.3 Shale Gas Capacity as Inferred from Selected Alberta Shale Samples 13
4.1.3.1 Overview 13
4.1.3.2 Results 13
4.2 X-Ray Diffraction, Petrographic Analysis and Electron Microscope Results 14
4.2.1 XRD Observations of the Banff-Exshaw Formation 14
4.2.2 Thin-Section Description of the Banff Formation 16
4.2.2.1 Sample 8688, Lower Banff, Well 00/06-24-084-07W6/00 16
4.2.2.2 Sample 6922, Middle Banff, Well 00/08-27-039-11W5/00 19
4.2.3 SEM/ESEM Description of the Banff Formation 19
4.2.3.1 Sample 8690, Lower Banff, Well 00/16-18-107-06W6/00 19
4.3 Permeametry Results 19
4.4 Mercury Porosimetry Results 20
4.5 Discussion of Analytical Results 21
5 Are There any Banff-Exshaw Shale Gas Wells in Alberta at Present? 22
6 References 23
Appendices 25
Appendix 1 – Cross-Sections 25
Appendix 2 – Descriptions of Outcrop Sections 28
Appendix 3 – Well Logs, Core and Type of Analysis Run on Each Sample 31

Tables

Table 1. Banff and Exshaw formations core locations 6
Table 2. Banff and Exshaw formations outcrop sample sites 6
Table 3. Analyses performed on shale samples and references for the methodologies 8
Table 4. Gas capacity data (as-received basis) 15

Table 5. Summary of permeametry results 21

Figures

Figure 1. Location of Banff Formation outcrop and subsurface core sample sites, and stratigraphic cross-sections 2
Figure 2. Stratigraphic chart of the Mississippian Banff Formation 3
Figure 3. Model of prograding carbonate ramps of the Banff Formation 3
Figure 4. Isopach from the top of the Banff Formation to the top of the Wabamun Formation 4
Figure 5. Stratigraphic cross-section B08 5
Figure 6. Stratigraphic cross-section B14 5
Figure 7. Banff Formation outcrop near Nordegg 7
Figure 8. Exshaw Formation type section underlying the lower Banff Formation at Jura Creek, near Canmore 7
Figure 9. a) Sample 8688, lower Banff Formation. b) Left photo: sample 8688, lower Banff Formation. Right photo: sample 8688, lower Banff Formation. c) Sample 8688, lower Banff Formation 17
Figure 10. a) Left photo: sample 6922, middle Banff Formation. Right photo: sample 6922, middle Banff Formation. b) Left photo: sample 6922, middle Banff Formation. Right photo: sample 6922, middle Banff Formation. c) Sample 6922, middle Banff Formation 18
Figure 11. Left photo: sample 8690, lower Banff Formation. Right photo: sample 8690, lower Banff Formation 19
Figure 12. Sample 8695, middle Banff Formation, well 100/08-08-76-07W6/00, depth 2911.8 m 22
Figure 13. Sample 6936, lower Banff Formation, well 100/04-23-72-10W6/00, depth 3565.2 m 22

Acknowledgments

The authors thank S. Rauschning, D. Lammie, M. Cohen and K. Henderson from the Department of Energy for their support of this project. D. Magee of Alberta Geological Survey provided expert help in preparing some of the figures, and our summer student M. Ahmed helped in many areas in preparing this report. Thanks to L. Wilcox of the ERCB Core Research Centre for her sampling assistance. Finally, we thank F. Hein and D. Cant for their help in the field and to F. Hein for editing the report.

Abstract

Alberta Geological Survey has started a project to quantify shale gas resources in the province by collecting 72 core samples and 59 outcrop samples from the Mississippian Banff and Exshaw formations. A series of 10 analyses was run on selected samples: isotherm, Rock Eval™ 6, total organic carbon (TOC), organic petrology, bulk mineralogy, clay mineralogy, permeametry, helium and mercury porosimetry, scanning electron microscopy, environmental scanning electron microscopy and thin section examination. Gas capacity has been calculated using a base case of 100% desorption, as well as a case assuming 25% free gas. A few thin sections and electron microscope descriptions are included, with the remainder becoming available when descriptions are complete.

To develop assessment units for Banff shale gas, regional stratigraphic cross-sections and maps of the Banff are being created. Two cross-sections and one map are included, with the remainder of the sections and maps to be released when they are completed.

1 Introduction

The purpose of this report is to introduce the reader to a shale gas sampling and analysis project that we completed in the spring of 2008. The present project encompasses sampling and analyzing the organic geochemistry and describing the sedimentology of the shales of the Colorado Group and Banff and Exshaw formations. This report presents the results for the Banff and Exshaw formations; the Colorado Group results are being released in a separate report (Rokosh et al., 2008b). A companion document introducing the shale gas assessment project in Alberta (Rokosh et al., 2008a) is also being released. The ultimate purpose of analyzing the shale of both the Banff and Exshaw formations and the Colorado Group is to assess resource potential. Datasets are being released as open file reports (Beaton et al., 2008a, b; Pawlowicz et al., 2008a, b) and will be available on the Alberta Geological Survey (AGS) website (www.ags.gov.ab.ca). Some of the data, such as thin sections and scanning electron microscope (SEM) photos, will be released when geological descriptions have been completed. The website is targeted for the public, government and industry, and will be expanded to include more data as it is generated.

In this report, we briefly review the stratigraphy of the Banff and Exshaw formations but stress that the stratigraphic framework we have published is a work in progress. We have chosen to release the results of our analyses prior to completion of the framework to make them available in a timely manner. We will continue to work on the framework and will release cross-sections and maps as they are completed. As the framework's purpose is to package shale for resource assessment, we do not necessarily follow traditional methods of correlation (i.e., sequence stratigraphic).

The stratigraphic summary in Section 2 is followed by a brief discussion of the methodology used in the analyses and highlights of the geochemical and sedimentological results. The latter section includes a summary and discussion of adsorption analyses and a preliminary calculation of resources associated with each analysis. We assume two scenarios in the resource calculation: a) adsorbed gas only with no free gas present, and b) adsorbed gas plus 25% free gas. We will be expanding upon the highlights with a more comprehensive analysis of results in the future and will publish these results as soon as possible.

2 Stratigraphy of the Banff and Exshaw Formations

In this section, we begin to construct a stratigraphic framework and review regional aspects of Banff and Exshaw formations stratigraphy (largely from prior publications). We have included two cross-sections and a map (Figure 1 and Appendix 1); the purpose of the cross-sections is to delineate the Banff shale into assessment units. The correlations and nomenclature (i.e., Banff 1B shale, etc.) used in this report are strictly informal, although in some cases we have followed sequence stratigraphic principles. Regional geological characteristics are briefly discussed, within which shale sedimentology and geochemistry will be assessed to evaluate the potential for shale resources. The 'science' of our discussion is necessarily brief and will be expanded as we apply data from this report and prior publications to regional mapping of shale geochemistry and geology.

2.1 Mississippian Banff and Exshaw Formations Stratigraphy

Banff shale (Figure 2) has been identified as a potential source rock (Smith and Bustin, 2000; Schmidt and Riediger, 2002; Stasiuk and Fowler, 2004) that may have complemented hydrocarbon generation within the Exshaw Formation. In southern Alberta, the lower Exshaw Formation shale, the Exshaw Formation siltstone and the lowermost Banff Formation shale are correlative with the lower, middle and upper Bakken Formation of Saskatchewan and North Dakota, respectively, according to Smith and Bustin (2000).

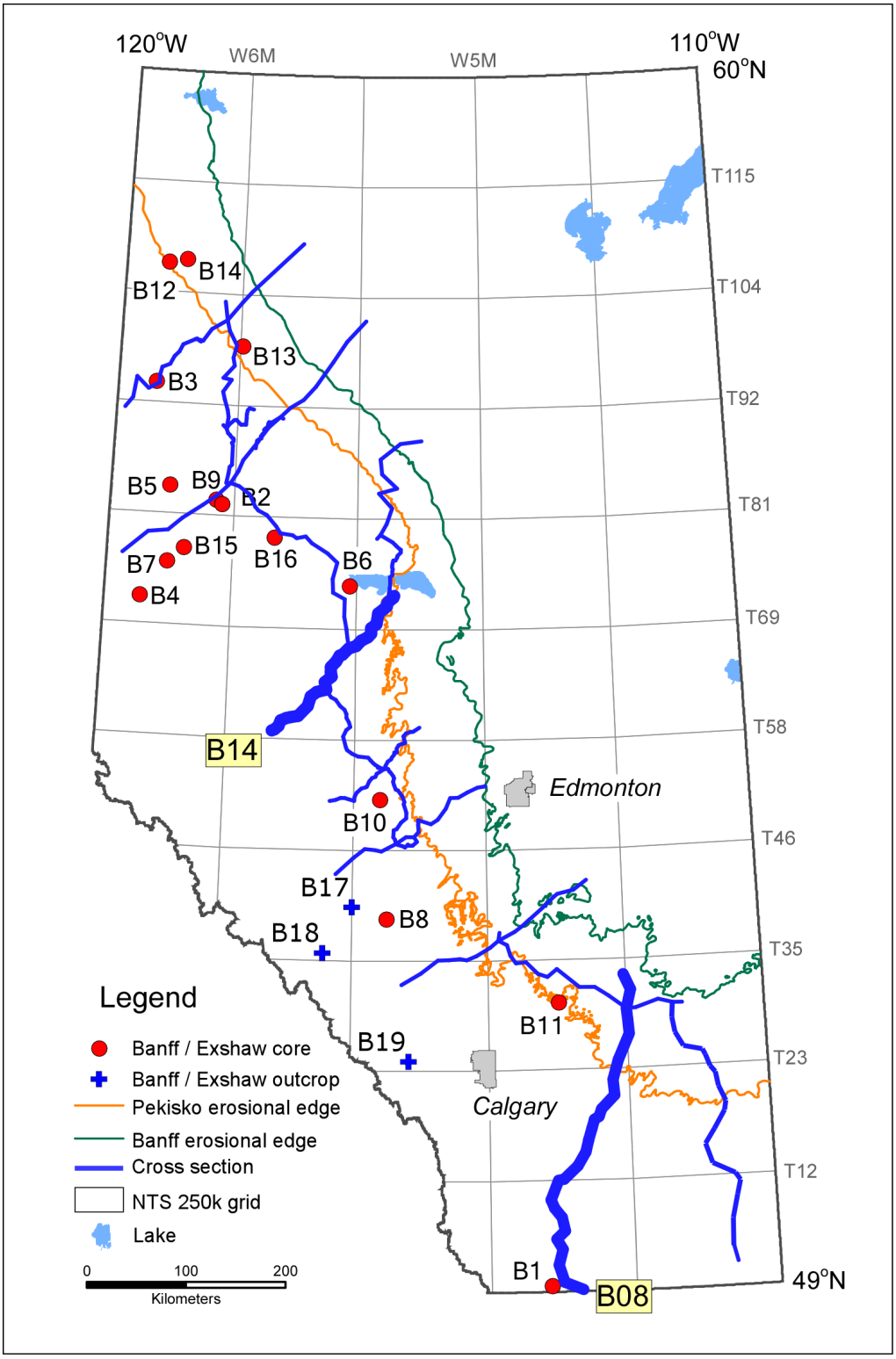

Figure 1. Location of Banff Formation outcrop and subsurface core sample sites, and stratigraphic cross-sections. A detailed list of the core and outcrop locations is provided in Tables 1 and 2. Stratigraphic sections use approximately one well every two to three townships. Cross-sections in bold lines have been included in this report. All other cross-sections are being refined and will be available when complete.

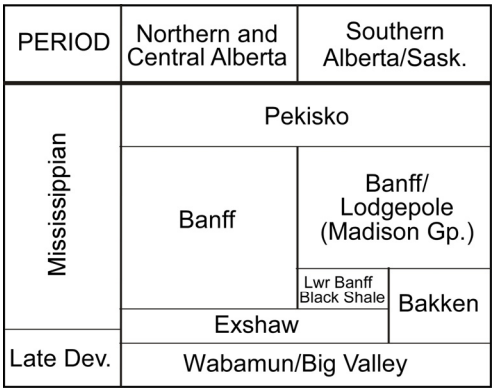

Figure 2. Stratigraphic chart of the Mississippian Banff Formation (*modified after* Richards et al., 1994; Smith and Bustin, 2000).

Prograding carbonate ramps overlie thick basinal shale in the Peace River Embayment, resulting in stacked successions of lower Banff Formation shale (maximum thickness of ~120–130 m) overlain by middle Banff Formation carbonate (>50 m thickness). Much of the Banff shale has low 'background' resistivity, with a higher argillaceous and carbonate mudstone component, compared to the underlying highly radioactive and organic black shale of the Exshaw and lower Banff formations. The lower Banff black shale (Figure 2) exhibits a resistivity increase in areas where it is close to the underlying, highly radioactive and highly organic Exshaw black shale succession. Of equal interest in evaluations of the Banff 'shale' is the argillaceous, organic-rich, lime mudstone (e.g., facies B in Figure 3) of the lower to middle Banff Formation. These rocks are not usually considered part of shale gas resource evaluations, having no known production from Alberta or the United States. We have taken a few samples of these units for evaluations of their future resource potential.

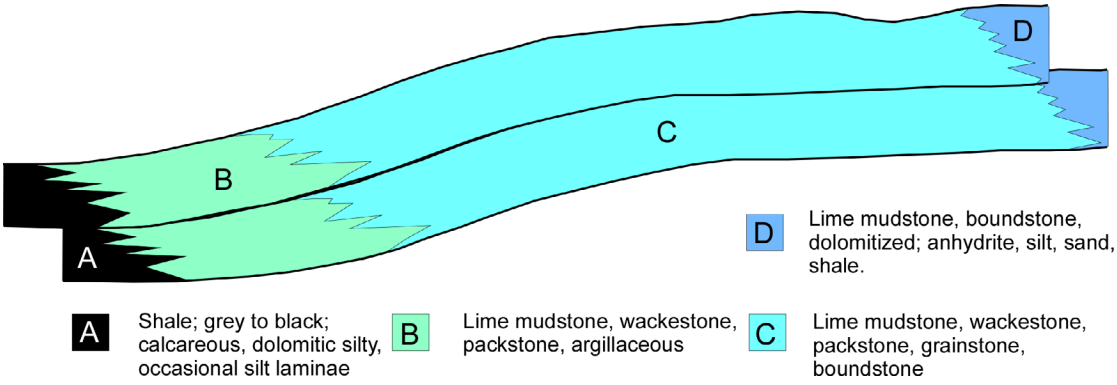

Figure 3. Model of prograding carbonate ramps of the Banff Formation (*modified from* Richards et al., 1994).

In the extreme southern part of the study area, lower Banff and Exshaw sedimentary rocks are present below thick Madison Formation carbonate and correlate with the productive Bakken Formation shale in the Williston Basin (Richards et al., 1994; Smith and Bustin, 2000). The Exshaw black shale in the extreme southeastern part of Alberta is generally less than ~5 m thick, with up to 14 wt. % total organic carbon (TOC); it apparently attains a maximum thickness of about 18 m in western Alberta (*see* Caplan, 1997). The lower Banff shale in the extreme southeast is a maximum of 1.5 m thick, containing up to 14 wt. % TOC (Smith and Bustin, 2000). Stasiuk and Fowler (2004) classified the organic facies of the Exshaw/Bakken Formation in southeastern Alberta as shallow-water facies with a transition to deeper water facies east of the Alberta-Saskatchewan border.

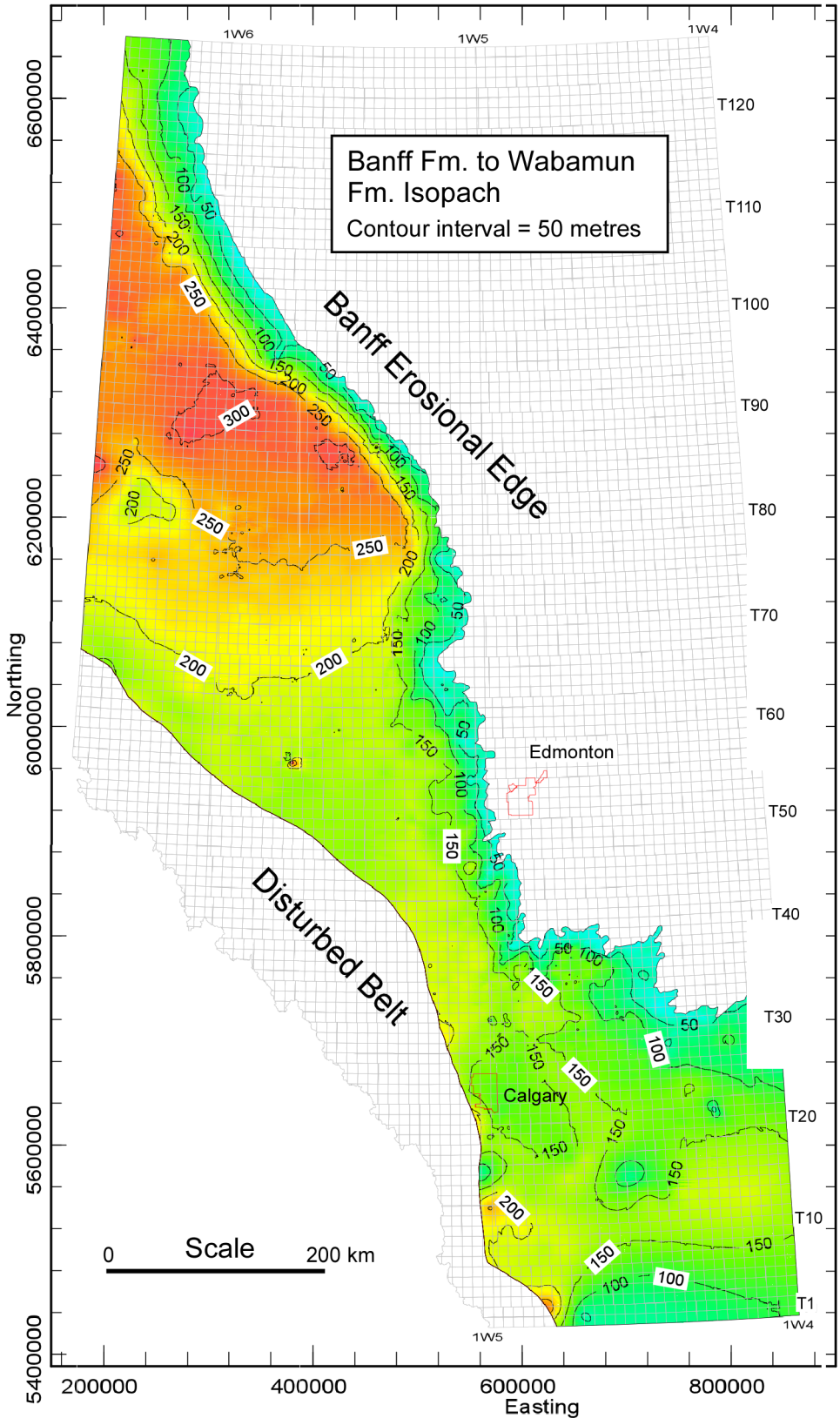

Figure 4. Isopach from the top of the Banff Formation to the top of the Wabamun Formation (50 m contour interval).

2.1.1 Banff Formation Stratigraphic Cross-Section B8 (64-10W5 to 54-25W5)

This west-to-east section (Figure 1 and, in the back of the report, Figures 4 and 5) shows the thickening of the Banff shale at the east end of the section where the isopach between the informal Banff 1B shale and the Wabamun Formation is about 125 m. The Banff 'B' argillaceous carbonate at the east end of the section is 20 m thick, is encased in the shale and represents a reasonably deep water carbonate-ramp facies prograding from the east, likely lower facies 'B' in Figure 3. The Banff 'B' thins westward, becoming more argillaceous, and downlaps onto 5 m of (presumably) Exshaw Formation shale. In general, Banff shale appears to be more calcitic and dolomitic, and less organically rich than the Exshaw shale; hence, it exhibits a lower gamma-ray value. Exceptions occur when Banff black shale overlies Exshaw shale. Farther to the east along the adjoining cross-sections, the shale immediately above the Banff 'B' thickens to more than 100 m.

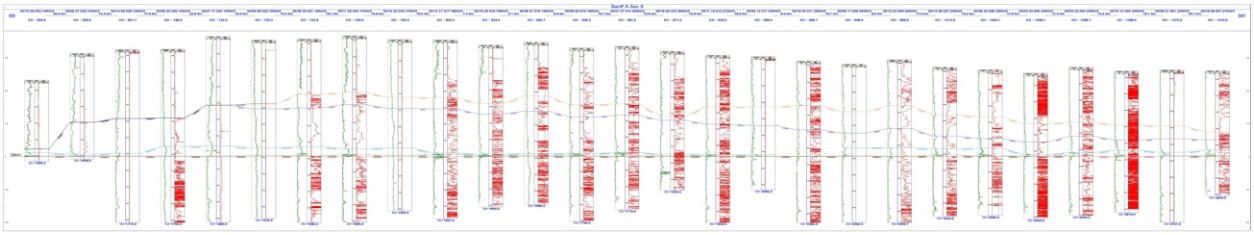

Figure 5. Stratigraphic cross-section B08. See Appendix 1 for a larger version.

2.1.2 Banff Formation Stratigraphic Cross-Section B14 (1-21W4 to 32-14W4)

This south-to-north section (*see* Figure 1 and, in the back of the report, Figure 6) traverses the Banff Formation beginning at the Alberta–United States border. Note the thick section of carbonate rocks overlying the Exshaw Formation where the Banff strata are part of the Madison Group. The Exshaw is very thin (<5 m) throughout the area and is not likely a shale gas target in itself. We have made a lithostratigraphic correlation of the shale in the lower Banff to highlight its distribution and thickness. At the south end of the section and near the north end, the lower Banff is much shalier and is correlative with the upper and possibly middle portions of the Bakken Formation of Saskatchewan (Smith and Bustin, 2000). The lower Banff in southeastern Alberta lies near the shoreline of the Williston Basin during Bakken time and does not contain the relatively thick black shale evident in the deeper parts of the Williston Basin.

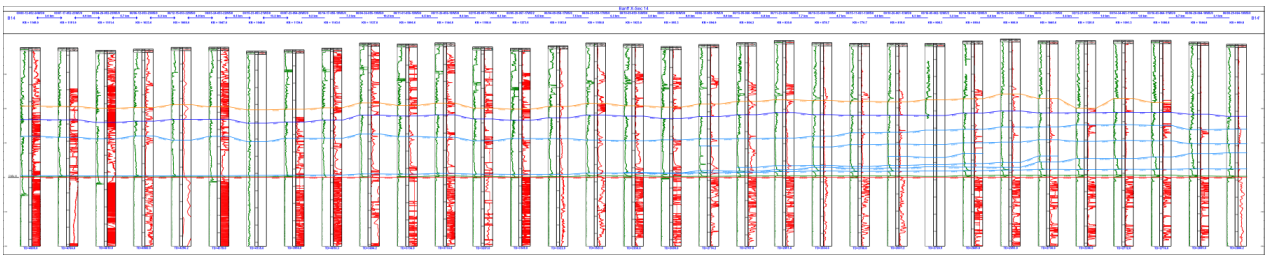

Figure 6. Stratigraphic cross-section B14. See Appendix 1 for a larger version.

There is little published information concerning the sedimentology and regional geochemistry of the lower Banff shale upon which to build a regional knowledge database concerning shale gas potential of this unit in Alberta. Shale gas potential of the Banff Formation is a work in progress and the data

generated herein will aid the identification of current and future resource potential. This is especially true of thicker shale successions in northwestern Alberta.

3 Methodology of Sampling and Testing

Samples were selected for analysis from outcrop and core (Figure 1, Tables 1, 2). Outcrop sampling of the Banff and Exshaw formations occurred at Nordegg and Jura Creek (Figures 7 and 8), for which site descriptions are given in Appendix 2. A single sample was taken in 2 m of dark shale, possibly in the upper Banff, at Kootenay Plains. Subsurface core was selected to determine both vertical and spatial geochemical and geological characteristics of the formation. Our approach to sampling and description of core was to spend a maximum amount of time and effort in sampling the core, resulting in a brief rather than full core description. We feel that maximum benefit at this early stage of shale gas evaluation in Alberta will be obtained by sampling and testing of core, while recognizing that the lack of a full description is a shortcoming in geological analysis. As stated by Schieber and Zimmerle (1998), such a small amount of research has been done on shale—let alone shale as a reservoir—that everyone is on a very steep learning curve. In our case, fully describing core from 16 wells would have greatly reduced the time and money available for sampling and analysis. Furthermore, the core is freely available at the ERCB Core Research Centre in Calgary, so all interested parties can view it at their leisure. From time to time, we will return to describe the core and will then make this information available.

Table 1. Banff and Exshaw formations core locations (*see also* Figure 1).

Site No.	Unique Well Identifier	Latitude (NAD83)	Longitude (NAD83)	Year Drilled	No. of samples	Formation
B01	100/01-20-001-24W4/00	49.045566	-113.165460	1981	3	Banff/Exshaw
B02	100/02-14-082-02W6/00	56.103477	-118.193028	1950	6	Banff
B03	100/02-28-094-09W6/00	57.179218	-119.376578	1952	6	Banff
B04	100/04-23-072-10W6/00	55.245950	-119.431068	1972	4	Banff/Exshaw
B05	100/06-04-084-07W6/00	56.252096	-119.047260	1974	2	Banff
B06	100/07-08-074-14W5/00	55.394566	-116.113837	1949	8	Banff/Exshaw
B07	100/08-08-076-07W6/00	55.568451	-119.040018	2002	2	Banff
B08	100/08-27-039-11W5/00	52.383168	-115.491096	1955	14	Banff
B09	100/08-30-082-02W6/00	56.135519	-118.293350	1985	3	Banff/Exshaw
B10	100/09-06-052-11W5/00	53.463004	-115.601615	1954	8	Banff/Exshaw
B11	100/12-36-030-22W4/00	51.614422	-112.978894	1950	4	Banff/Exshaw
B12	100/15-05-107-08W6/00	58.264601	-119.290939	2001	4	Banff
B13	100/15-27-098-25W5/00	57.539368	-117.965423	2002	1	Banff
B14	100/16-18-107-06W6/00	58.296137	-118.982929	1954	2	Banff
B15	100/16-24-077-06W6/00	55.693279	-118.777249	1986	3	Banff
B16	102/06-02-079-22W5/00	55.817907	-117.332954	1984	2	Banff

Table 2. Banff and Exshaw formations outcrop sample sites (*see also* Figure 1).

Site No.	Datum	UTM Zone	Easting	Northing	Site Location Name	No. Samples	Formation
B17	NAD83	11	567642	5816426	Nordegg - railroad section	30	Banff, Exshaw
B18	NAD83	11	539339	5769916	Kootenay Plains - mountain section	1	Banff?
B19	NAD83	11	628902	5661581	Jura Creek—Exshaw Type Section	28	Banff, Exshaw

Figure 7. Banff Formation outcrop near Nordegg. Up section is to the left; arrows are about 2 m in length. See Appendix B for outcrop description and sample locations.

Figure 8. Exshaw Formation type section underlying the lower Banff Formation at Jura Creek, near Canmore. The Exshaw black shale (arrow) is about 9 m thick. See Appendix 2 for outcrop description and sample locations.

Our sample strategy in outcrop was to select at least one sample for each facies or lithological change, or, if the lithology was vertically congruent over a few metres, to select enough samples to give a reasonable vertical and, if possible, lateral distribution of characteristics. Where permitted, approximately 0.3–0.6 m of surface material was unearthed in order to obtain samples that may be less affected by surficial weathering. If the outcrop face was well indurated, then a surface sample was selected. As there is a relative lack of shale core in the Western Canada Sedimentary Basin (WCSB), subsurface core selection was guided primarily by the availability of core rather than by the strategic selection of samples. A key core sampling issue is that the amount of sample selected from each core is limited; thus, the number of tests and types of tests that can be performed are restricted. Energy Resources Conservation Board

personnel approved the size and number of samples selected from each core. Although ideal, it was not possible to subject all samples to every analysis. We have attempted to obtain a reasonable temporal and spatial distribution of characteristics in both formations and have tried not to test core on which the same analyses have already been carried out at a similar depth, as indicated in published reports (e.g., Smith and Bustin, 2000; Stasiuk and Fowler, 2004). An important point concerning the core samples is that all sample depths are recorded as core depths rather than being converted to log depths.

Our experience in unconventional gas resource analysis, conversations with industry and background research led to the selection of more than 10 geochemical and geological analyses to perform on outcrop and subsurface samples (Table 3). This suite of analyses has been carried out on many low-permeability and organic-rich samples, as indicated in a variety of public reports. Only a brief description of each type of analysis performed on the samples and the rationale for selecting the analysis is given here. We urge the reader to consult the publication or website listed in Table 3 for a more detailed description of each analytical method, and to gain an understanding of the methodology and potential errors involved in the analyses.

Table 3. Analyses performed on shale samples and references for the methodologies.

Type of Analysis	Company/Analyst	Notes and Reference
Isotherm	Schlumberger; CBM Solutions	References available upon request
Mercury porosimetry, envelope and helium pycnometry	Department of Physics, University of Alberta (D. Schmitt)	(Webb and Orr, 1997).
Permeametry	Department of Earth and Atmospheric Sciences, University of Alberta (M. Gingras)	Gingras et al. (2004)
Rock Eval™ 6 /TOC	Geological Survey of Canada; Schlumberger; CBM Solutions	Peters (1986); Peters and Cassa (1994); Lafargue et al. (1996)
Organic petrography	Geological Survey of Canada	Taylor et al. (1998)
Petrographic analysis (thin section)	Vancouver Petrographics; CBM Solutions	
Scanning electron microscope (SEM) with energy-dispersive x-ray (EDX)	Department of Earth and Atmospheric Sciences, University of Alberta (G. Braybrook)	http://easweb.eas.ualberta.ca/page/29
Environmental scanning electron microscope (ESEM)	Department of Biology, University of Alberta (R. Bhatnagar)	http://www.biology.ualberta.ca/facilities/microscopy/?Page=2146
X-ray diffraction (bulk and clay mineral)	SGS Minerals Services Ltd. (H. Zhou); CBM Solutions Ltd.	Klein (2002)

3.1 Rock Eval™ 6 and Total Organic Carbon (TOC)

A fundamental property of shale gas reservoirs is organic richness. Rock Eval™ 6 (Rock Eval is a registered trademark of Institut français du pétrole) is a test of the maturity of the organic matter. All other factors being equal, a higher organic content is generally preferred in shale gas plays because more gas may be generated.

3.2 Organic Petrology

Organic petrology examines organic macerals and determines the source of the organic matter (i.e., marine or terrestrial). Macerals in organic petrology are akin to minerals in sedimentology. Furthermore, during gas desorption, the shape and morphology of organic matter may contribute to permeability and influence gas diffusion rates (although this is a relatively new area of research).

3.3 Isotherm (Adsorption) Analysis

Adsorption analysis identifies the maximum amount of gas that a shale sample may hold. However, the maximum capacity may not represent the present state of storage of the reservoir. See Section 4 for an explanation of this test.

3.4 X-Ray Powder Diffraction (XRD) and Whole-Rock and Clay Mineralogy

X-ray powder diffraction (XRD) identifies the mineralogy of a sample by means of a characteristic scattering or diffraction pattern generated by an electromagnetic beam (x-ray) on a crystal. X-ray diffraction analysis and interpretation and x-ray fluorescence spectroscopy (XRF) on core samples were done by SGS Minerals Services Ltd. (www.ca.sgs.com), while CBM Solutions Ltd. (www.cbmsolutions.com) performed XRD analysis and interpretation on outcrop samples. A detailed summary of sample preparation procedures and scan conditions for XRD and XRF will be provided upon request.

SGS Minerals uses a Siemens D5000 diffractometer with cobalt radiation and Siemens search-match software for peak identification. Mineral proportions are based on relative peak heights and may be strongly influenced by crystallinity, structural group or preferred orientations (H. Zhou, SGS Minerals Services Ltd., pers. comm., 2008). The calculation of mineral abundances from both bulk-mineral analysis and clay-mineral separates is based on relative peak intensity and is reconciled with a whole-rock analysis by x-ray fluorescence spectroscopy. The detection limit of minerals is approximately 0.5–2.0 wt. % according to SGS, but can be as high as 3–5 wt. % (www.xrd.us). However, amorphous compounds are not detected by XRD.

CBM Solutions uses a Siemens D5000 or D500 with copper or cobalt x-ray tube with search-match software for peak identification. X-ray diffraction results were analyzed using a commercial Rietveld program for quantification of the mineralogy. The accuracy of the Rietveld analyses is considered to be ±3% in minerals with fixed cell dimensions. In samples with substantial amounts of disordered clay minerals, the total percentage of clay was determined by Rietveld fitting and then the relative abundances of the clay species were quantified by integrating the areas under the 00l peak. The Lorentz and polarization contributions to the x-ray intensity in this study were corrected following the procedures of Pecharsky and Zavalij (2003, p. 192). As a result of the presence of disordered phases and the need for a combination of methodologies, the accuracy of the results varies sample by sample. For samples in which substantial montmorillonite, random mixed-layer clays and/or degraded illite are present, the percentage mineralogy reported here is best considered semiquantitative (*summarized from* CBM Solutions Ltd. 2008).

3.5 Petrographic Analysis (Thin Section)

Thin sections, cut by Vancouver Petrographics (www.vanpetro.com), were used to analyze mineralogy, texture, fracturing, microfabric and microstratigraphy. Not all thin sections contain an upper glass cover. Most of the samples were cut by saw using water as a cooling/lubricant liquid; in some cases, however, a limited amount of kerosene was used during the preparation due to the presence of swelling smectite that would have caused excessive swelling of the sample. Once the samples were completed, the polished surfaces were cleaned with acetone. All thin sections were impregnated with Petropoxy™ 154 (http://burnhampetrographics.com/petropoxy/ppp.php#154).

3.6 Permeametry

Permeability is one of the critical parameters characterizing potential shale gas reservoirs; furthermore, the identification of shale seals or lack of permeability is an equally important parameter in shale gas exploration and pool delineation. Spot permeametry analysis will determine the permeability to gas (nitrogen in our case) of the selected samples. Note that the diameter of a nitrogen molecule is about 0.15 nanometre (nm; 1.5 ångstroms), whereas the diameter of a methane molecule is about 0.4 nm (4.0 ångstroms). Spot permeametry analysis was performed at the University of Alberta under the guidance of M.K. Gingras, under ambient conditions on a portable probe permeameter (CoreLabs model PP-250) with nitrogen as the pore fluid. Optimal accuracy of the model is between about 0.01 and 3000 millidarcies (mD; ±1%). Five or six measurements were made on each sample. The highest and lowest values were excluded and an average taken of the remainder; however, all measurements are included in the data release. No corrections were applied to the data.

3.7 Mercury Porosimetry and Helium Pycnometry

Mercury porosimetry and helium pycnometry are techniques for quantifying intrusion pore diameter, total pore volume, surface area, and envelope and skeletal densities of the sample. A helium gas molecule is smaller than a methane molecule, whereas mercury is larger than a methane molecule; hence, the pore characteristics of the samples are relatively well described although not accurate relative to a methane molecule, and the methods provide detailed information on the micro-, meso- and macroporosity and/or seal characteristics of the samples. Porosimetry and pycnometry analyses were done at the University of Alberta under the direction of D. Schmitt. Some of the samples desorbed gas; hence, the samples were put under vacuum in a cold oven prior to analysis.

3.8 Scanning Electron Microscope (SEM) and Environmental Scanning Electron Microscopy (ESEM)

Both of these instruments are being used to characterize the microfabric of the samples, and the morphology, size and distribution of the pores. The scanning electron microscope (SEM) can also provide a mineralogical analysis (energy-dispersive x-ray, EDX), as well as backscattered images on selected samples. All samples are coated with gold prior to analysis.

Samples viewed with the environmental scanning electron microscope (ESEM) were examined in high vacuum mode using a secondary electron detector operating at 15–20 kV with a Philips/FEI XL 30 ESEM. The ESEM equipment has a resolution of 2.5 nm and a magnification of up to 200 000×. The SEM is a JEOL 6301F (field-emission scanning electron microscope) with magnification ranging from 20 to 250 000×. Semiqualitative elemental analysis (EDX) is available via a PGT x-ray analysis system. The resolution of EDX mineralogical analysis is ~1 μm diameter.

4 Shale Gas Data Analysis

Seventy-two core samples and 59 outcrop samples from the Banff and Exshaw formations were selected for analyses (*see* Figure 1, Tables 1, 2). The selection of all subsurface core samples received the approval of the ERCB Core Research Centre. Energy Resources Conservation Board rules state that a copy of all data from core must be sent to the Core Research Centre. This section examines a few of the analytical techniques and highlights specific aspects of the formations that reflect on their potential, or lack thereof, for shale gas resources. Any further interpretation of the results will be published in journals or as AGS open file reports. All data will be made available on the AGS website (www.ags.gov.ab.ca).

4.1 Geochemistry Results

Tabulated data and photographic images for the organic petrography are available in Beaton et al. (2008b).

4.1.1 Organic Geochemistry as an Indicator of Shale Gas Potential

Geological evidence overwhelmingly indicates that the majority of economic hydrocarbon (oil and gas) deposits originated from the breakdown of organic matter, such as marine and lacustrine phytoplankton and terrestrial vegetation. Marine settings are favourable for the accumulation of large amounts of sediments and organic matter. Some terrestrial environments are also well suited to preserving organic matter (peat and coal). Preserved organic matter can be subsequently incorporated into lithified sediment and undergo thermal maturation with burial. Maturation causes physical and chemical changes in the organic matter, generating and releasing hydrocarbons, the nature of which is determined by the original organic matter. Furthermore, microbial activity can contribute significant amounts of gas (biogenic methane) in sediments.

Hydrogen is the key element in determining petroleum potential of sediment. Marine-type organic material (plankton, algae) has high ratios of hydrogen to carbon, whereas terrestrial material (trees, vegetation, etc) has higher oxygen to carbon ratios. When these compounds break down, they are likely to produce (initially) more oil and gas, respectively.

Overwhelmingly, the shale samples contain marine plankton and algae as the dominant organic component. Mature samples show evidence of thermal breakdown of organic matter, suggesting that hydrocarbons have been generated by the samples. The presence of marine organic matter and degraded organic matter suggests that the samples have hydrocarbon potential.

These geological processes may result in shale that contains small amounts of organic matter derived from different sources. The subsequent processes of deposition, decomposition and burial, accompanied by increasing heat and pressure, cause the organic matter to undergo physical and geochemical changes that include a progressive loss of oxygen and a generation of hydrocarbon from the partial breakdown of the remaining organic material, or kerogen. This promotes a large reduction in the H/C ratio as the kerogen becomes increasingly aromatic, and the resultant hydrocarbon is released. This stage of hydrocarbon generation reflects oil generation within the 'oil window' and, with increasing depth of burial and temperature, the processes continue, subsequently causing further breakdown of the kerogen and the production of gas. Furthermore, previously generated oils may now be broken down into gas. The physical and geochemical changes experienced by organic matter as it goes through deposition, preservation, burial and breakdown are referred to as 'maturation.' The degree of maturation indicates whether organic matter has passed through the oil or gas window, and is used as an exploration tool. The geochemistry of organic matter, including the relative amounts of H and O associated with organic matter in the rocks, can also be used to indicate the original type of organic matter in the rock and the respective hydrocarbon potential, as different organic materials have different hydrocarbon potentials.

A common method for evaluating the hydrocarbon potential of a source rock is the Rock Eval^{TM} analysis. This method involves combusting a small amount of sample (100 mg) in a controlled environment and analyzing the produced gas. The sample is heated to 300°C in an oxygen-purged environment. This temperature volatilizes the in-place hydrocarbon, known as the 'S1' hydrocarbon. The temperature of the Rock Eval apparatus is then slowly increased to a final temperature of approximately 600°C. During this time, the remaining kerogen starts to break down, resulting in generation and release of hydrocarbons. This is referred to as the 'S2' hydrocarbon and represents the total remaining hydrocarbon potential of the source rock. The total source-rock potential is determined as the sum of S1 and S2. The temperature at which the maximum amount of S2 hydrocarbon is generated is referred to as T_{max} (maximum temperature), which has been correlated with other maturation parameters (such as vitrinite reflectance)

and is considered a good maturation indicator. A T_{max} between 435°C and 450°C indicates that the sample is in the oil window; temperatures below or above these represent immature or gas prone rocks, respectively.

The Rock Eval process also records evolved CO_2 derived from the volatilization of hydrocarbons throughout the analysis to determine the oxygen content of the organic matter. Subsequently, the sample is combusted in the presence of air at 600°C. Evolved CO_2 is determined and added to the volatilized hydrocarbon CO_2 to determine total organic carbon (carbonate carbon does not break down at this temperature, but siderite, if present, may partially break down.

Key indicators of shale gas potential include the amount of organic matter within a potential source rock, the level of maturation or 'cooking' of the organic matter and the type of organic matter.

A greater total amount of organic matter will increase the hydrocarbon potential of a source rock. Total organic matter is indicated by the total organic carbon (TOC) value. Shale with TOC values as low as 0.5–1 wt. %, and carbonate rocks with as little as 0.5 wt. % TOC, can act as a source rock. Source rocks from Canada range from 1.5% to 25% TOC, with most in the range 3% to 7%.

Organic matter derived from marine sediments can include plankton, marine algae, bacteria and lipid-rich components of higher plants (spores, waxes, etc). These materials are hydrogen rich (hydrogen/carbon ratios of 1.4–1.6, hydrogen index >700) and are oil prone. Organic matter derived from plant material is hydrogen poor (H/C ratio 1.3–1.5) and is more gas prone.

The PI (production index) is calculated using S1/(S1+S2) and indicates the amount of hydrocarbon that has been produced relative to the total amount that can be produced.

4.1.2 Results of the Analysis

This study tested a wide variety of samples from outcrop and core to obtain an overview of lateral and vertical compositional characteristics of shale-bearing intervals from the Banff and Exshaw strata. Within each outcrop section or core, an attempt was made to sample a variety of lithological variations, including black shale, associated grey shale, siltstone, and some sandstone and even carbonate. Samples were analyzed using Rock Eval™ 6 pyrolysis to determine hydrocarbon potential.

4.1.2.1 Banff Formation

The Banff Formation was subdivided into upper, middle and lower portions. The upper Banff samples consisted mainly of limestone and lime mudstone/shale. These samples generally had low TOC, typically <0.2 wt. %, indicating poor source-rock potential. Middle Banff samples had somewhat higher TOC values, in the order of 0.5 wt. %, indicating that this laminated siltstone and lime mudstone has somewhat greater source-rock potential than the upper Banff, although its potential is still limited. Lower Banff samples consisted of black shale, black calcitic shale, grey shale and laminated shale (i.e., with siltstone). Calcitic shale and grey shale typically were low in TOC (<0.5 wt. %); however, black shale ranged from 0.7 to 3.3 wt. %. These values suggest the black shale packages in the lower Banff have sufficient TOC (although on the low side) to have source-rock potential. The T_{max} values are typically in the 450°C – 470°C range, indicating they are within the gas-generation window. With depth, Banff shale becomes overmature.

4.1.2.2 Exshaw Formation

The Exshaw Formation black shale is known to have high TOC and is a well-known source rock in the Western Canadian Sedimentary Basin (WCSB). Immediately underlying the lower Banff shale, the combined interval of Banff shale and Exshaw shale may provide a source-rock package with acceptable thickness to warrant further shale gas investigations. Exshaw TOC values range from 1.3 to 4.6 wt. %,

well within the typical range of known source rocks in the WCSB. Values of T_{max} in the 430–460°C range suggest that the Exshaw Formation, where sampled, was approaching the top of the oil window and just entering the gas window.

4.1.3 Shale Gas Capacity as Inferred from Selected Alberta Shale Samples

4.1.3.1 Overview

Gas content results for shale in Alberta are very limited and often are not clearly identified as to the producing horizon, or whether shale and associated silt and sand are being coproduced. An alternative approach to determining gas content in shale is to evaluate gas-holding capacity and draw inferences on content potential. Gas capacity can be determined using adsorption isotherms. In this procedure, a sample is crushed and subsequently equilibrated to maximum adsorptive capacity with the gas of choice (in this case methane). The sample is allowed to slowly adsorb as much gas as possible at a given temperature, over a range of pressures, to mimic reservoir conditions. The experimental data from the adsorption is modelled using Langmuir equations relating equilibrium pressure and volume of gas adsorbed experimentally to anticipated reservoir pressure. The results allow a prediction of the maximum gas capacity of the sample at reservoir conditions.

Organic matter has a great capacity to adsorb gas owing to a relatively large surface area derived from its microporous nature, not unlike that of activated charcoal. Gas can be held on the surface of organic matter by physical or chemical forces. Gas capacity will therefore be related to the amount of organic matter present (as indicated by TOC). Furthermore, gas adsorption capacity increases with increasing maturity of the organic matter, but capacity decreases with increasing reservoir temperature. Primarily, the large surface area of organic matter dictates adsorption capacity. Illite and smectite also have a high surface area, relative to kaolinite and quartz, and can add to the adsorption capacity of shale.

As is the case with coal, organic matter tends to generate more gas than it can retain via adsorption; therefore, the maximum holding capacity of the shale is a fair proxy for anticipated gas in the sample (if the sample is assumed to be at saturation). Furthermore, it has been demonstrated that pore spaces and fractures in gas shale typically contain free gas, which is gas derived, and perhaps subsequently expelled, from the organic matter. This gas is thought to represent anywhere from 25% to 50% of gas produced in a shale gas well, so the maximum gas content of a shale determined by an adsorption isotherm analysis may under-represent the total gas available for production in a shale play.

4.1.3.2 Results

Adsorption analysis results are presented in Table 4**.** Isotherms are available in Beaton et al. (2008b). Variations in mineralogy, total organic carbon, lithology, thickness, depth and maturation within a shale formation prevent extrapolation of a few maximum gas capacity estimates from approximately 20 wells and outcrop to a basin-wide, regional scale. Here, calculations of gas capacity are presented for the individual wells and extrapolated to a maximum gas content on a Bcf/square mile basis.

Using typical shale thickness, as observed in the sample wells, the gas capacity was determined using Langmuir isotherm analysis. Average shale density of 2.5 g/cc was used in the calculations. Two sets of results are presented, the maximum capacity and the maximum capacity plus 25% of capacity to account for potential free gas in the system. The results assume saturation to the capacity of the shale matrix. These results are very preliminary and additional analyses are needed to validate the predictions of gas capacity.

Samples from the Exshaw have a capacity in the range 0.2–0.9 cc/g. Lower Banff samples also have a low capacity (0.2 cc/g).

Total gas capacity (Bcf/square mile) is determined by thickness of the shale package as well as the unit gas capacity of the shale package. Table 4 indicates average thickness for the given unit across Alberta. Although shale gas capacity is rather low, the thickness of shale units can make a play more feasible. Furthermore, shale has varying TOC content within a given formation, and this is reflected in the gas capacity of the sample. These points are both shown by the thick Lower Banff grey shale versus the thinner Lower Banff black shale. Although the cumulative grey shale thickness is in the order of 100 m, the gas capacity is lower than that of the thinner black shale, giving the two intervals similar total gas capacity according to our calculations.

It should be noted that the thicknesses indicated in Table 4 and used for calculations are averaged. Across Alberta, the thickness of shale packages, as well as total organic content (TOC) and maturation (T_{max}) are highly variable; therefore, it is important to obtain a large number of data points to capture the variability before making gas capacity estimates and inferring resource potential.

4.2 X-Ray Diffraction, Petrographic Analysis and Electron Microscope Results

Four techniques were used to determine mineralogy and microfabric in the samples: x-ray diffraction (XRD), scanning electron microscopy (SEM), energy dispersive x-ray analysis (EDX) and petrographic analysis (thin section). The use of the terms upper Banff, lower Banff and middle Banff are informal. Here we briefly summarize some key observations from three of our methods of analysis. Scanning electron microscope images and descriptions are available in Pawlowicz et al. (2008b). Thin-section descriptions and images are provided in Section 4.2.2. X-ray diffraction data are available in Pawlowicz et al. (2008b).

4.2.1 XRD Observations of the Banff-Exshaw Formation

Banff Formation mineralogy in the subsurface is generally characterized by high contents of quartz (13–51 wt. %) and muscovite (3–27 wt. %), with varying percentages of calcite (0–62 wt. %), dolomite (0–34 wt. %) and orthoclase (0–23 wt. %). A distinct similarity between the upper and lower Banff Formation is the low quantity of clay minerals; if clay minerals are present, they are usually palygorskite and, more rarely, illite. The relative lack of clay minerals may suggest that many of the samples analyzed were from facies ‘B’ in Figure 3, some of which are classified as argillaceous lime mudstone and generally exhibit a lower gamma-ray reading on well logs than shale. Banff shale (i.e., high clay-mineral content) is generally present at the extreme base of the Banff sedimentary column, resting directly on Exshaw shale. The most noticeable difference between upper and lower Banff mineralogy is the greater percentage of carbonate minerals in the lower Banff. Major minerals in the lower Banff Formation are quartz, muscovite and calcite, while quartz, muscovite and orthoclase are the major minerals in the upper Banff, with only a trace of carbonate minerals. There are also mineralogical differences between northern and southern Alberta in the lower Banff Formation. Relative to samples in northern Alberta, an increase in secondary dolomitization and a decrease in calcite are observed in the south.

Outcrop samples of the Banff Formation were taken at Nordegg in the central Cordilleran foothills, and on Jura Creek in the southern Cordilleran mountains (Figures 1, 7, 8). Middle Banff samples, taken only at Nordegg, have a high percentage of calcite (34–91 wt. %) and quartz (4–53 wt. %), with variable amounts of dolomite (0–30 wt. %), illite (0–21 wt. %) and ankerite (0–37 wt. %). Lower Banff samples at both sites have high quartz (28–39 wt. %) and calcite (10–41 wt. %), with orthoclase (5–20 wt. %) and illite (3–11 wt. %) and a variable percentage of dolomite (0–30 wt. %). The only discernible difference between lower Banff samples from the two sites is a higher percentage of calcite (at least 9 wt. %) in samples from Jura Creek (in comparison to Nordegg).

Samples were taken from the Exshaw Formation at both Jura Creek and Nordegg. Major minerals are quartz (7–82 wt. %), calcite (1–37 wt. %), orthoclase (1–71 wt. %) and illite (0–43 wt. %). Nordegg

Table 4. Gas capacity data (as-received basis).

Sample	Depth (m)[1]	Analysis Temperature (°C)	Average Thickness of Shale (m)	Moisture (wt. %)	Langmuir Pressure (MPa)	Langmuir Volume (standard cubic cm/g)	Density	Unit	T_{max} (°C)	TOC (wt. %)	Calculated Reservoir Pressure (MPa)	Calculated Gas Volume at Reservoir Pressure (cc/g)	Gas Capacity (Bcf/sq. mi.)	
													Max. Capacity on Organic Matter	Max. Capacity + 25% (for Free Gas)
Core samples														
8678/79	1994.5	50	30	1.42	9.42	1	2.5	banff	436	1.66	19.5461	0.7	4.6	5.8
8684/85	1975.0	50	100	0.66	8.29	0.3	2.5	banff	436	0.44	19.355	0.2	4.8	6.0
Outcrop samples														
6517	2500	38	8	0.77	5.2	0.86	2.558	jc.exshaw		4.48	24.5	0.7	1.3	1.7
6525	2500	38	8	1.87	12.2	1.07	2.583	jc.exshaw		nd	24.5	0.7	1.3	1.7
6534	2000	38	2	1.47	17.17	1.13	2.589	nord.exh	554	3.25	19.6	0.6	0.3	0.4
6543	2500	38	2	0.59	15.27	0.66	2.352	nord.banff	320	0.75	24.5	0.4	0.2	0.2
6548	2500	38	2	1.51	24.57	1.14	2.608	nord.banff		0.09	24.4	0.6	0.3	0.3

Core samples		**Outcrop samples**	
Banff 8678/79 (00/08-30-082-02W6/00)	Lower Banff black shale	jc.exshaw	Exshaw black shale at Jura Creek Outcrop Site
Banff 8684/85 ((00/02-14-082-02W6/00)	Lower Banff grey shale	nord.exh	Exshaw black shale at Nordegg Outcrop Site
		nord.banff	Banff black shale at Nordegg Outcrop Site

samples have a higher quartz and orthoclase content than those from Jura Creek. Outcrop samples exhibit an increase in clay and carbonate minerals and a decrease in mica and feldspar, relative to subsurface samples.

Banff Formation samples were further analyzed for mineralogy, texture and structure using thin-section analysis (i.e., petrography), complemented by SEM imaging and EDX analysis. Thin sections were prepared for 25 core samples. Two petrographic samples (8688, 00/06-24-084-07W6/00, Figure 9; 6922, 00/08-27-039-11W5/00, Figure 10) and one SEM photo (8690, 00/16-18-107-06W6/00, Figure 11) are discussed here. All other thin-section descriptions and photos will be released in an AGS open file report and on the AGS website (http://www.ags.gov.ab.ca/) when complete.

Three significant observations resulted from the thin-section analysis:

1) The lower Banff sample shows a considerable amount of quartz and mica (muscovite, according to XRD analysis) in thin section, whereas the middle Banff sample has an increase in carbonate minerals (particularly dolomite), similar to the XRD data.
2) The presence of silt-sized grains within stacked sheets of mica enhances permeability. This is also seen in the permeametry results discussed in the next section.
3) The lower Banff sample exhibits thin (~2 silt grains thick) porous laminations that are discontinuous, whereas the middle Banff sample appears massive due to secondary calcite cement, quartz overgrowths and a greater degree of dolomitization.

4.2.2 Thin-Section Description of the Banff Formation

4.2.2.1 Sample 8688, Lower Banff, Well 00/06-24-084-07W6/00

Sample 8688 was taken at a core depth of 2247.3 m (7373 ft.) from well 100/06-04-084-07W6/00. The sample is a dark brown mudstone with very fine silt laminae that are laterally discontinuous (Figure 9a). The matrix is composed mainly of clay-sized grains (Figure 9a, 9b) with very fine to fine silt-sized grains dispersed throughout the matrix. The silt-sized grains (light coloured in Figure 9a, b) are subrounded with minor euhedral carbonate crystals present. A moderate shale microfabric is defined by the alignment of clay-sized grains and is oriented parallel to bedding. The larger grains comprise quartz and feldspar (light coloured in Figure 9a, left photo and purple-blue in Figure 9c), along with some shell detritus and minor carbonate crystals.

Magnification 2.5× (Figure 9a): Discontinuous silty laminations occur within a dark clay mudstone. The laminations appear to have a sharp base and top, and are less than 5 μm thick, except in a few local areas along the laminations. A few microfractures are present (upper third of Figure 9a) parallel to bedding, but may have formed during core retrieval or sample preparation, since the hand sample fractured upon cutting.

Magnification 20.0×: Under high magnification, a moderate fabric defined by clay-sized grains is observed (northwest to southeast in Figures 9b, c). In addition to the silt laminae (upper right in Figure 9b, c), silt-sized grains are evenly dispersed throughout the mudstone. Under cross-polarized light (Figure 9b, right photo), quartz cement is observed, particularly within the silt laminations. The cement occludes about 50%–60% of the porosity in the laminations. The subrounded to subangular opaque matter (Figure 9b, left photo) is likely framboidal pyrite (based on morphology) and is unevenly distributed throughout the sample.

a)

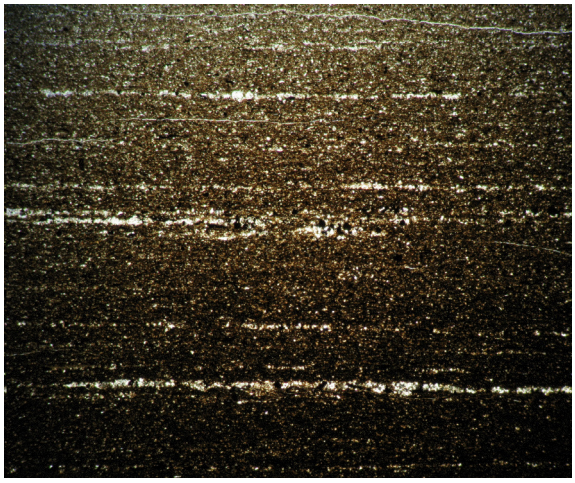

b)

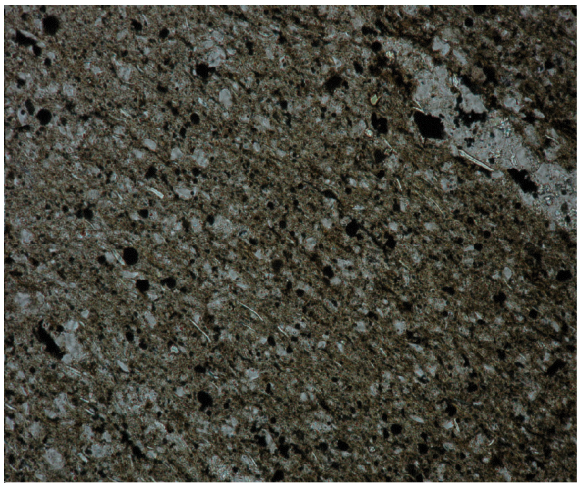

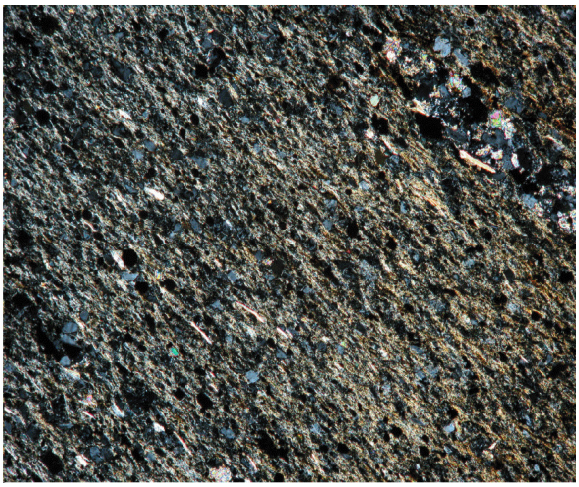

c)

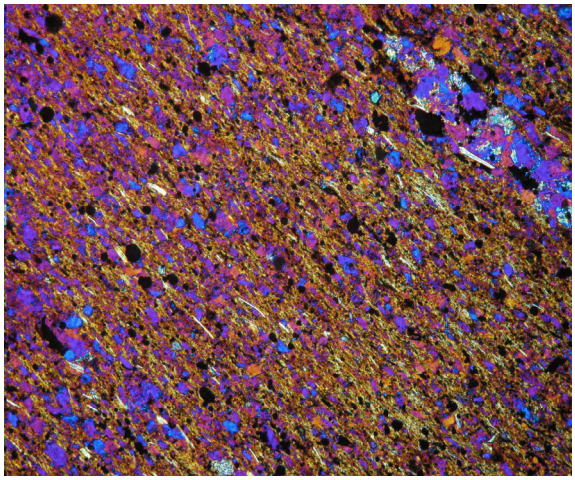

Figure 9. a) Sample 8688, lower Banff Formation, Tx_8688_01 (plane-polarized light, mag. 2.5x). b) Left photo: sample 8688, lower Banff Formation, Tx_8688_09 (plane-polarized light, mag. 20.0x). Right photo: sample 8688, lower Banff Formation, Tx_8688_10 (cross-polarized light, mag. 20.0x). c) Sample 8688, lower Banff Formation, Tx_8688_11 (plane-polarized light, mag. 20.0x) with quartz plate inserted.

a)

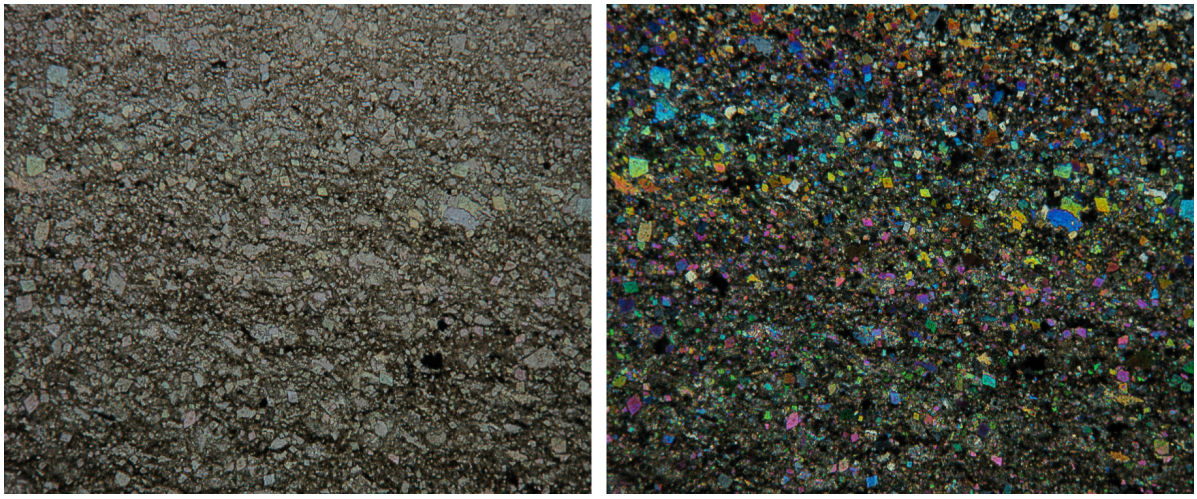

b)

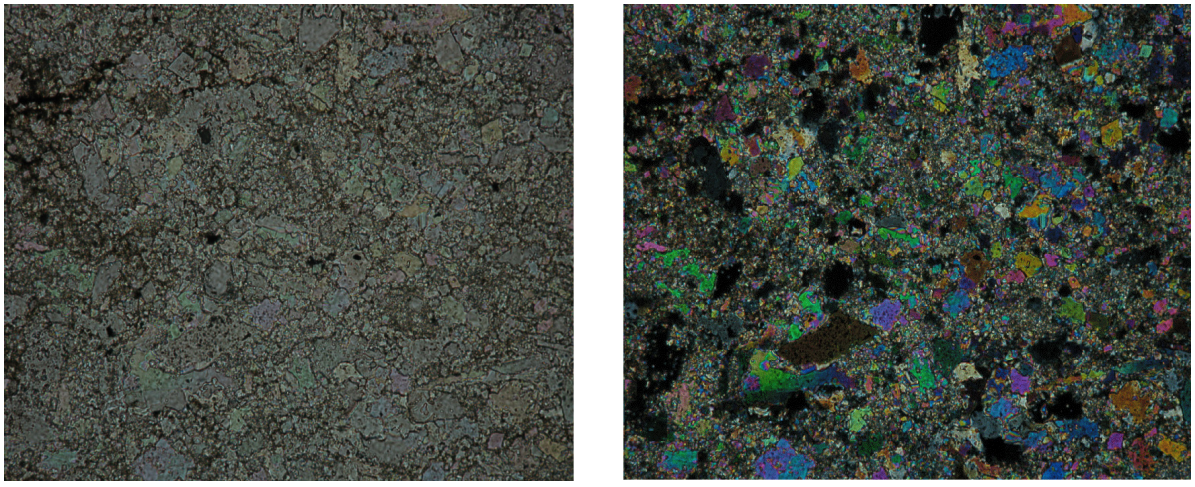

c)

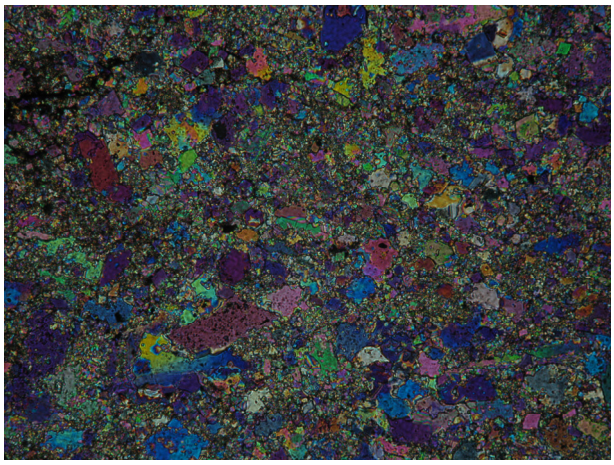

Figure 10. a) Left photo: sample 6922, middle Banff Formation, Tx_6922_07 (plane-polarized light, mag. 10.0x). Right photo: sample 6922, middle Banff Formation, Tx_6922_08 (cross-polarized light, mag. 10.0x). b) Left photo: sample 6922, middle Banff Formation, Tx_6922_13 (plane-polarized light, mag. 20.0x). Right photo: sample 6922, middle Banff Formation, Tx_6922_14 (cross-polarized light, mag. 20.0x). c) Sample 6922, middle Banff Formation, Tx_6922_15 (quartz plate inserted, mag. 20.0x).

4.2.2.2 Sample 6922, Middle Banff, Well 00/08-27-039-11W5/00

Sample 6922 was taken at a core depth of 3706.4 m (12,160 ft.) from well 100/08-27-039-11W5/00. It is a laminated (Figure 11a, right photo), dolomitic lime mudstone. The micritic matrix is composed of clay and calcium carbonate. Less than 5% silt-sized, detrital quartz grains are present and dispersed in the matrix. Calcite cement and dolomitization in this sample are pervasive and fabric destructive. Dolomitization occurs in the form of euhedral, rhombohedral crystals (Figure 10b, c). The dolomitization has occurred to a greater degree where laminations are present. In addition to calcite cement and dolomitization, this sample contains secondary quartz and pyrite.

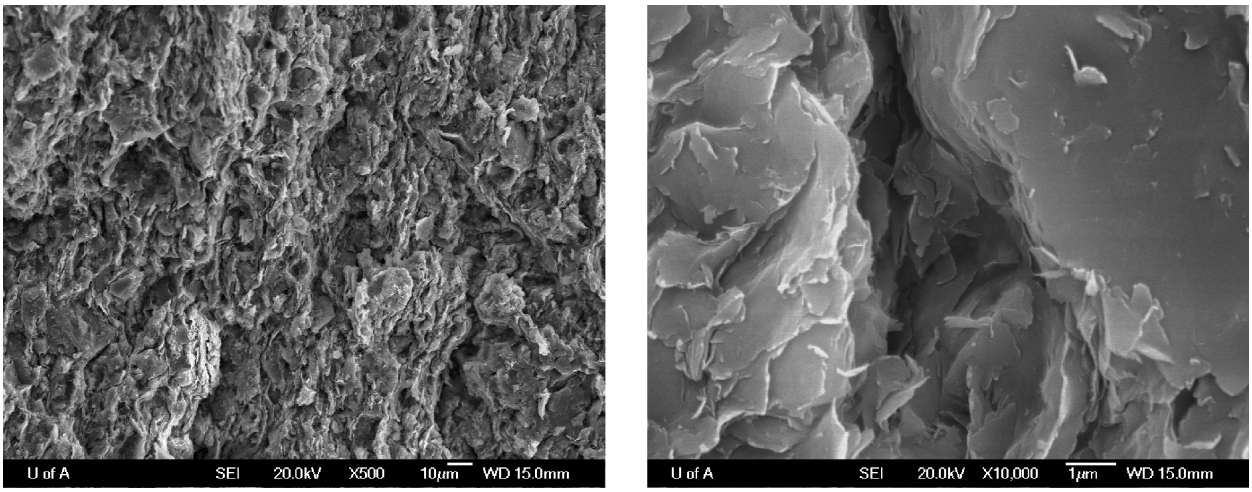

Figure 11. Left photo: sample 8690, lower Banff Formation, scanning electron microscope image 8690S_02. Right photo: sample 8690, lower Banff Formation, scanning electron microscope image 8690S_04. Note the difference in scale of the two photos.

4.2.3 SEM/ESEM Description of the Banff Formation

4.2.3.1 Sample 8690, Lower Banff, Well 00/16-18-107-06W6/00

Sample 8690 was taken from the upper part of the lower Banff Formation at a core depth of 621.2 m (2038 ft.) in well 100/16-18-107-06W6/00 (Figure 11). The sample on the left is turned on its side so that up is to the west-northwest. The photo on the left shows that the sample consists of very well compacted clay sheets with a long axis trending north-northeast. Very fine silt-sized grains are randomly distributed and are embedded in the matrix, with clay sheets compacted around them. Energy-dispersive x-ray mineralogical analysis indicated that very few carbonate minerals are present. The clay mineralogy is a mixture of muscovite/biotite and illite/smectite. The silt-sized grains are largely quartz, with framboidal pyrite as a minor constituent. Microporosity seems to be quite high with, as seen in the right photo, a relatively rare macropore measuring greater than 3–5 μm in diameter.

4.3 Permeametry Results

The permeametry results are very encouraging and, in fact, some of the numbers are quite spectacular. The results are summarized in Table 5 and, along with the raw data, are available in Pawlowicz et al. (2008a). However, all of the single-phase measurements were done at ambient conditions and no corrections were applied, so results at reservoir conditions may differ considerably (Miller et al., 2007). Samples were carefully chosen to exclude fractured sediment, although microfractures may still be present. Bustin (2007) suggested that the minimum permeability in a shale gas reservoir should exceed 0.00001 mD (= 10^{-8} darcies) and, in fact, all the results exceed this value. These results are also consistent

with the quoted permeability from producing shale gas reservoirs (e.g., Davies and Vessell, 2002 for Ohio Shale and Lewis Shale; *see also* Bustin, 2007) and, from that point of view, are very encouraging.

The permeability results for the Banff Formation range from about 0.002 to 0.65 mD (Table 5) with one high value of 3.775 mD, although it may be due to microfracture generation during core deloading (*see* Section 4.2.2.1). All five measurements of this sample yielded consistent results, but microfractures viewed in thin section appear to be due to unloading. We will investigate this sample further using SEM results. Other samples also yielded fairly high results, such as sample 8691 (well 100/16-24-077-06W6/00) that has a miniperm value of 0.965 mD.

Shale is heterogeneous on the micro scale, so variations in vertical and horizontal permeability are expected. Furthermore, it is difficult to detect microfractures that may form in a sample after it has been brought to surface (i.e., unloading fractures), although natural microfractures can also develop in the subsurface and open up when the rock is brought to the surface. Microfractures may considerably enhance permeametry results; hence, the results would not represent reasonably accurate values.

Any discussion of these results must be tempered with the realization that the numbers quoted in Table 5 were determined from small pieces of shale (approximately 1 cm^3) and therefore do not necessarily represent regional permeability trends. What is not determined here is both the vertical and lateral extent of the enhanced shale permeability zones and the silt laminae (if these exist). These high-permeability zones appear to be thin enough to be hidden on well logs and would appear to be below minimum log resolution. Nevertheless, there may be more than one thin, highly permeable zone in a 50 m shale package, for example; therefore, identifying and determining the number and lateral extent of these zones may be very important to the completion, production and economics of shale gas reservoirs.

4.4 Mercury Porosimetry Results

A brief analysis of two of the samples is presented here; a complete tabulation of the data is available in Pawlowicz et al. (2008a). Here, mercury porosimetry is used to determine the macropore throat diameter (>50 nm or 0.05 μm) of a sample and a large portion of the mesopore throat diameter range (2–50 nm or 0.002–0.05 μm), but cannot determine micropore throat diameters (<2 nm; Bustin 2007; http://www.iupac.org). For reference, a molecule of gas is about 0.38 nm in diameter, which is an order of magnitude below the capability of mercury porosimetry (~2–3 nm or 0.02–0.03 μm). We have included all the data points in our graphs (Figures 12, 13), even though a few data points on each side of the graph are artifacts of the testing procedure and may not identify the diameter of pore throats.

Both the lower Banff sample (Figure 13) and the middle Banff sample (Figure 13) display similar features. Firstly, the dominant peak at about 100 μm in both graphs represents surface features and may not be a real pore. The graph suggests the samples essentially have little or no macroporosity or mesoporosity. From the point of view of shale gas resources, this is not a good result in that the meso-sized and macro-sized pore throats are closed due to compaction and/or cementation and there may be a few large pores present. The SEM discussion in Section 4.2.3, however, clearly identifies a Banff sample with a large amount of microporosity. If we assume other results to be relatively accurate (i.e., permeametry), they suggest that, indeed, there are permeable Banff shale units. Both of the samples used here are largely tight rocks or seals at the meso- and macroporosity scale.

Table 5. Summary of permeametry results.

AGS Sample No.	Core Depth (feet)[1]	Core Depth (m)[2]	Unique Well Identifier	Formation	N	Average permeability (mD)[3]	Average permeability (mD)
6919	12000.0	3657.6	100/08-27-039-11W5/00	U. Banff	5	0.648333	
6937	11710.5	3569.2	100/04-23-072-10W6/00	Exshaw/L. Banff	5	0.965	
8691		2612.75	100/16-24-077-06W6/00	L. Banff	5	0.0020667	
6923	12245.0	3732.3	100/08-27-039-11W5/00	M. Banff	6	0.0031325	
6924	12399.0	3760.9	100/08-27-039-11W5/00	M. Banff	5	0.139	
6925	12441.0	3792.0	100/08-27-039-11W5/00	L.–M. Banff	5	0.0203667	
6928	12468.0	3800.2	100/08-27-039-11W5/00	L. Banff	6	0.004228	
6933		2795.3	100/01-20-001-24W4/00	Exshaw	5	0.153	
6935	11668.0	3556.4	100/04-23-072-10W6/00	L. Banff	5	0.002147	
6941	3803.0	1159.2	100/07-08-074-14W5/00	Banff	6	0.04575	
8682	6440	1962.9	100/02-14-082-02W6/00	L. Banff	6	0.0086025	
8688	7373	2247.3	100/06-04-084-07W6/00	L. Banff	6	3.775	
8693		2610	100/16-24-077-06W6/00	L. Banff	6, 3	0.003488	0.013 (layers)

[1] original units

[2] original and converted units

[3] Average permeability (K) for each sample is calculated by removing the high and low recorded values, then averaging the remaining values. Normally, five to six readings were taken on each sample. Contact AGS for a list of the raw results.

4.5 Discussion of Analytical Results

The Banff samples indicate both a good-news and bad-news shale gas scenario. There appears to be some fairly high permeability (Table 5), assuming the results are not due to a poor seal or the presence of microfractures. This is a significant result, considering that the samples were taken at depths of up to 3800 m. The porosimetry data, however, clearly show the presence of shale seals at the macro- and mesoporosity scale, although sample 8695 (Figure 13) suggests that a small volume of mesoporosity is present. Perhaps the low porosity is not surprising considering the depth of the samples, especially sample 6936. However, it is evident that the lowest part of the Banff Formation, along with the Exshaw Formation, is organic-rich and exhibits shale gas potential in other areas (as indicated in the gas capacity results of Table 5). The distribution and thickness of these zones will be mapped in the future and summarized in an AGS report. Less potential may exist in the thick, low-organic grey shale.

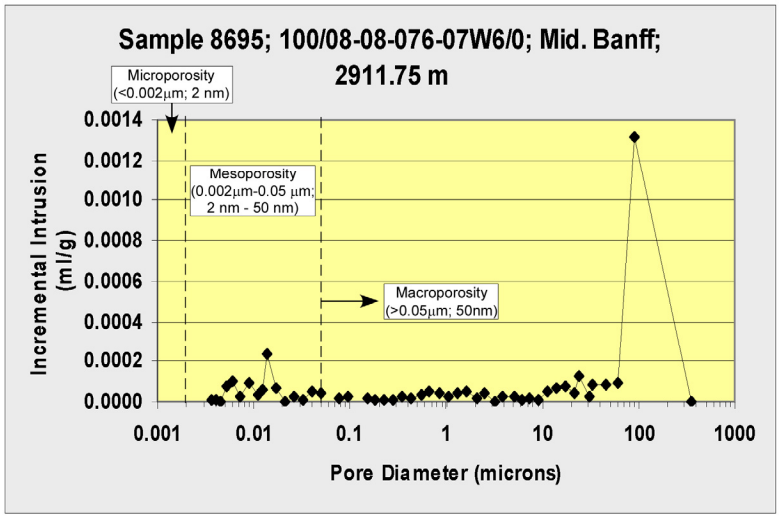

Figure 12. Sample 8695, middle Banff Formation, well 100/08-08-76-07W6/00, depth 2911.8 m.

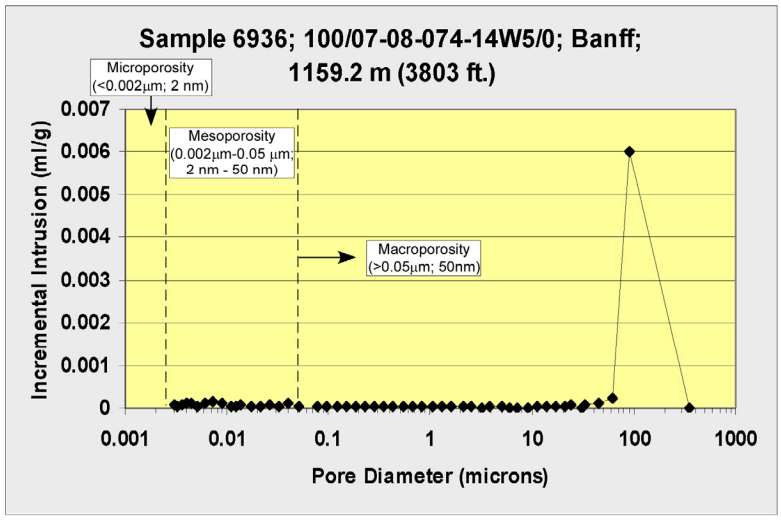

Figure 13. Sample 6936, lower Banff Formation, well 100/04-23-72-10W6/00, depth 3565.2 m.

5 Are There any Banff-Exshaw Shale Gas Wells in Alberta at Present?

To date, there are no known producing wells in the lower Banff Formation shale, although there are certainly wells that exhibited shows of hydrocarbons on gas chromatographs during drilling. For example, (assuming the data are correct) well 8-8-76-7W6 shows a gas kick in the lower Banff and Exshaw formations on the log of the gas chromatograph, while driller's notes on well 1-20-1-24W4 indicated gas in the Banff Formation. Although these may not be significant gas shows, they should be taken as an indication that gas is present and there are data that can be used to help assess shale gas resources in the Banff and Exshaw formations.

6 References

Beaton, A.P., Pawlowicz, J.G., Anderson, S.D.A. and Rokosh, C.D. (2008a): Rock Eval™, total organic carbon, adsorption isotherms and organic petrography of the Colorado Group: shale gas data release; Energy Resources Conservation Board, ERCB/AGS Open File Report 2008-11, 88 p.

Beaton, A.P., Pawlowicz, J.G., Anderson, S.D.A. and Rokosh, C.D. (2008b): Rock Eval™, total organic carbon, adsorption isotherms and organic petrography of the Banff and Exshaw formations: shale gas data release; Energy Resources Conservation Board, ERCB/AGS Open File Report 2008-12, 65 p.

Bustin, R.M. (2007): Gas shale reservoirs: reservoir access and gas in place; Canadian Society of Petroleum Geologists, Technical Luncheon, October 25, 2007, URL <www.cspg.org/events/webcasts/2007-webcasts.cfm> [November 2008].

Caplan, M.L. (1997): Factors influencing the formation of organic rich sedimentary facies: example from the Devonian–Carboniferous Exshaw Formation, Alberta, Canada; Ph.D. thesis, University of British Columbia, 688 p.

CBM Solutions Ltd. (2008): Mineralogical analyses by x-ray diffraction on an AGS sample suite; summary report prepared by CBM Solutions Ltd. for Energy Resources Conservation Board/Alberta Geological Survey, 5 p. plus tables.

Davies, D.K. and Vessell, R.K. (2002): Gas production from non-fractured shale; *in* Depositional Processes and Characteristics of Siltstones, Mudstones and Shale, E.D. Scott and A.H. Bouma (ed.), GCAGS Siltstone Symposium 2002, Gulf Coast Association of Geological Societies (GSAGS) Transactions, v. 52, p. 112–125.

Gingras, M.K., Mendoza, C.A. and Pemberton, S.G, (2004): Fossilized worm burrows influence the resource quality of porous media; AAPG Bulletin, v. 88, no.7, p. 875–883.

Klein, C. (2002): Manual of Mineral Science (22nd ed.); John Wiley and Sons, New York, 641 p.

Lafargue, E., Espitalié, J., Marquis, F. and Pillot, D. (1996): ROCK EVAL 6 application in hydrocarbon exploration, production and in soil contamination studies, Fifth Latin American Congress on Organic Chemistry, Cancun, Mexico, October 6–10, 1996.

Miller, M., Lieber, B., Piekenbrock, G. and McGinness, T. (2007): Low permeability gas reservoirs – how low can you go?; InSite, v. 2, p. 25–35.

Pawlowicz, J.G., Anderson, S.D.A., Rokosh, C.D. and Beaton, A.P. (2008a): Mineralogy, permeametry, mercury porosimetry and scanning electron microscope imaging of the Colorado Group: shale gas data release; Energy Resources Conservation Board, ERCB/AGS Open File Report 2008-14, 97 p.

Pawlowicz, J.G., Anderson, S.D.A., Rokosh, C.D. and Beaton, A.P. (2008b): Mineralogy, permeametry, mercury porosimetry and scanning electron microscope imaging of the Banff and Exshaw formations: shale gas data release; Energy Resources Conservation Board, ERCB/AGS Open File Report 2008-13, 59 p.

Pecharsky, V.K. and Zavalij, P.Y (2003): Fundamentals of powder diffraction and structural characterization of minerals; Kluwer Academic Publishers, New York, 713 p.

Peters, K.E. (1986): Guidelines for evaluating petroleum source rocks using programmed pyrolysis; American Association of Petroleum Geologists Bulletin, v. 70, p. 318–329.

Peters, K.E. and Cassa, M.R. (1994): Applied source rock geochemistry; *in* The Petroleum System – from Source to Trap, L.B. Magoon and W.G. Dow (ed.), American Association of Petroleum Geologists, Memoir 60, p. 93–117.

Richards, B.C., Barclay, J.E., Bloch, J., Bryan, D., Hartling, A., Henderson, C.M. and Hinds, R.C. (1994): Carboniferous strata of the Western Canada Sedimentary Basin; *in* Geological Atlas of the Western Canada Sedimentary Basin, G.D. Mossop and I. Shetsen (comp.), Canadian Society of Petroleum Geologists and Alberta Research Council, Special Report 4, URL <www.ags.gov.ab.ca/publications/wcsb_atlas/atlas.html> [February 2009].

Rokosh, C.D., Pawlowicz, J.G., Berhane, H., Anderson, S.D.A. and Beaton, A.P. (2008a): What is shale gas? An introduction to shale gas resource assessment in Alberta; Energy Resources Conservation Board, ERCB/AGS Open File Report 2008-08, 27 p.

Rokosh, C.D., Pawlowicz, J.G., Berhane, H., Anderson, S.D.A. and Beaton, A.P. (2008b): Geochemical and sedimentological investigation of the Colorado Group for shale gas potential: initial results; Energy Resources Conservation Board, ERCB/AGS Open File Report 2008-09, 86 p.

Schieber, J. and Zimmerle, W. (1998): Introduction and overview: the history and promise of shale research; *in* Shales and Mudstones (Volume 1): Basin Studies, Sedimentology and Paleontology, J. Schieber, W. Zimmerle and P. Sethi (ed.), Schweizerbart'sche Verlagsbuchhandlung, Stuttgart, Germany, p. 1–5.

Schmidt, M.J. and Riediger, C. (2002): An evaluation of the hydrocarbon potential of the Mississippian Banff Formation; CSPG Annual Convention, Calgary, Alberta, June 3-7 2002.

Smith, M.G. and Bustin, R.M. (2000): Late Devonian and Early Mississippian Bakken and Exshaw black shale source rocks, Western Canada Sedimentary Basin: a sequence stratigraphic interpretation; AAPG Bulletin, v. 84, p. 940–960.

Stasiuk, L.D. and Fowler, M.G. (2004): Organic facies in Devonian and Mississippian strata of Western Canada Sedimentary Basin: relation to kerogen type, paleoenvironment, and paleogeography; Bulletin of Canadian Petroleum Geology, v. 52, no. 3, p. 234–255.

Taylor, G.H., Teichmüller, M., Davis, A., Diessel, C.F.K., Littke, R. and Robert, P. (1998): Organic Petrology; Gebrüder Borntraeger, Berlin, Germany, 704 p.

Webb, P.A. and Orr, C. (1997): Analytical Methods in Fine Particle Technology; Micromeritics Instrument Corporation Publishers, Norcross, Georgia, 301 p.

Appendices

Appendix 1 – Cross-Sections

Figure 5. Stratigraphic cross-section B08.

Figure 6. Stratigraphic cross-section B14.

Banff X-Sec 8

B8 — B8'

02/10-29-032-14W4/0	00/06-27-029-15W4/0	00/14-08-028-14W4/0	00/08-22-026-15W4/0	00/07-11-024-15W4/0	00/06-33-021-16W4/0	00/11-02-020-17W4/0	00/15-17-017-18W4/0	00/16-25-016-19W4/0	00/08-21-016-19W4/0	00/08-30-015-19W4/0	00/01-27-014-20W4/0	00/16-20-013-20W4/0	00/11-16-012-21W4/0	00/06-12-011-23W4/0	00/16-05-011-23W4/0	00/06-17-009-24W4/0	00/10-22-008-24W4/0	00/12-28-007-23W4/0	00/06-22-006-23W4/0	00/03-34-005-24W4/0	00/03-32-004-23W4/0	00/14-14-003-24W4/0	00/08-31-001-23W4/0	00/16-06-001-21W4/0
30.2 km	15.3 km	17.6 km	22.9 km	25.8 km	18.7 km	28.3 km	7.4 km	5.1 km	8.6 km	10.7 km	10.8 km	14.8 km	18.9 km	6.0 km	18.7 km	8.5 km	11.0 km	12.3 km	11.8 km	11.5 km	14.5 km	16.1 km	20.7 km	
KB = 835.6	KB = 959.6	KB = 841.7	KB = 798.9	KB = 734.0	KB = 742.8	KB = 793.5	KB = 843.3	KB = 833.5	KB = 860.7	KB = 848.2	KB = 861.0	KB = 871.2	KB = 923.0	KB = 996.6	KB = 986.7	KB = 958.6	KB = 969.9	KB = 1014.8	KB = 1004.7	KB = 1096.1	KB = 1094.7	KB = 1186.0	KB = 1270.9	KB = 1319.8
TD=1265.0	TD=1408.0	TD=1715.0	TD=1700.0	TD=1860.5	TD=1690.0	TD=1995.0	TD=1637.0	TD=1604.0	TD=1690.0	TD=1700.0	TD=1719.0	TD=1632.0	TD=1849.0	TD=2065.0	TD=2280.0	TD=2592.3	TD=2395.7	TD=2340.0	TD=2382.0	TD=2555.0	TD=2400.0	TD=2610.0	TD=2701.0	TD=2054.0

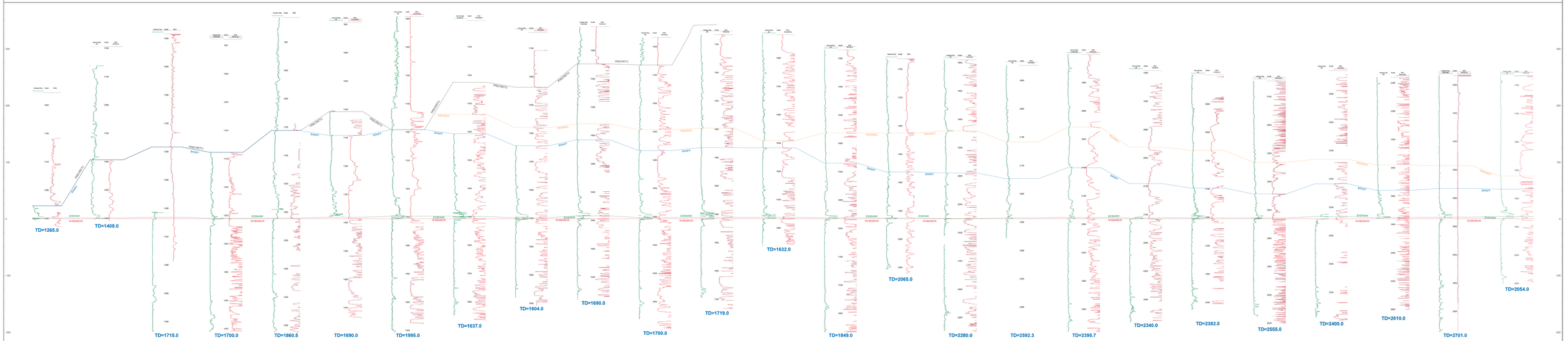

Banff X-Sec 14

	00/08-12-052-24W5/0	00/07-17-052-23W5/0	00/04-26-052-23W5/0	00/06-12-053-23W5/0	00/12-15-053-22W5/0	00/03-24-053-22W5/0	00/07-23-054-20W5/0	00/14-17-055-19W5/0	00/04-36-055-19W5/0	00/11-01-056-18W5/0	00/11-26-056-18W5/0	02/15-09-057-17W5/0	00/05-28-057-17W5/2	00/04-09-058-17W5/0	00/06-25-058-17W5/0	00/10-09-059-16W5/0	00/03-14-059-16W5/0	00/06-33-059-15W5/0	00/13-05-060-14W5/0	00/11-23-060-14W5/0	00/10-33-060-13W5/0	00/15-11-061-13W5/0	00/10-26-061-13W5/0	00/14-16-062-12W5/0	00/15-03-063-12W5/0	00/06-20-063-11W5/0	02/12-27-063-11W5/0	00/14-34-063-11W5/0	00/16-03-064-11W5/0	00/06-20-064-10W5/0	00/08-29-064-10W5/0	
B14	3.0 km	4.9 km	5.7 km	6.3 km	4.0 km	20.9 km	9.2 km	7.3 km	10.1 km	6.5 km	8.6 km	4.3 km	4.5 km	7.5 km	6.3 km	3.0 km	8.9 km	8.0 km	6.8 km	7.7 km	4.7 km	4.8 km	8.9 km	6.6 km	7.4 km	3.6 km	1.9 km	1.8 km	6.7 km	2.1 km		B14'
	KB = 1145.0	KB = 1151.9	KB = 1151.4	KB = 1023.6	KB = 1068.0	KB = 1047.0	KB = 1139.4	KB = 1143.6	KB = 1127.8	KB = 1096.6	KB = 1144.8	KB = 1158.0	KB = 1273.5	KB = 1183.8	KB = 1158.8	KB = 1023.0	KB = 893.3	KB = 894.9	KB = 804.2	KB = 820.8	KB = 878.7	KB = 770.7	KB = 815.6	KB = 890.6	KB = 986.9	KB = 1045.6	KB = 1125.5	KB = 1091.3	KB = 1086.8	KB = 1044.8	KB = 959.8	

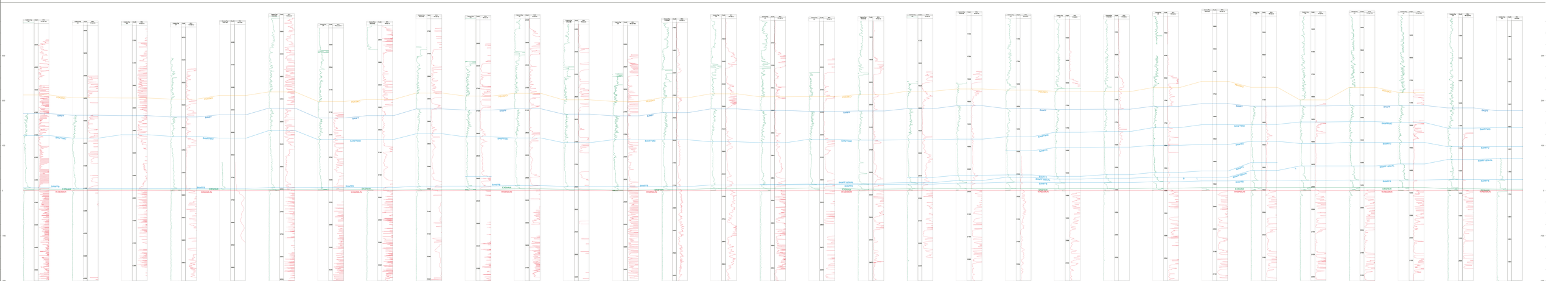

	TD=4809.0	TD=4766.0	TD=4610.0	TD=4500.0	TD=4296.2	TD=4319.0	TD=3950.0	TD=4010.3	TD=3694.2	TD=3736.0	TD=3733.8	TD=3281.0	TD=3149.0	TD=3322.9	TD=3523.8	TD=2930.0	TD=2699.0	TD=2714.2	TD=2707.0	TD=2851.4	TD=2834.6	TD=2700.0	TD=2601.2	TD=2685.0	TD=2693.0	TD=2730.0	TD=2246.0	TD=2712.0	TD=2716.0	TD=2655.0	TD=2804.2	

Appendix 2 – Descriptions of Outcrop Sections

Jura Creek Exshaw type section

Nordegg Banff section

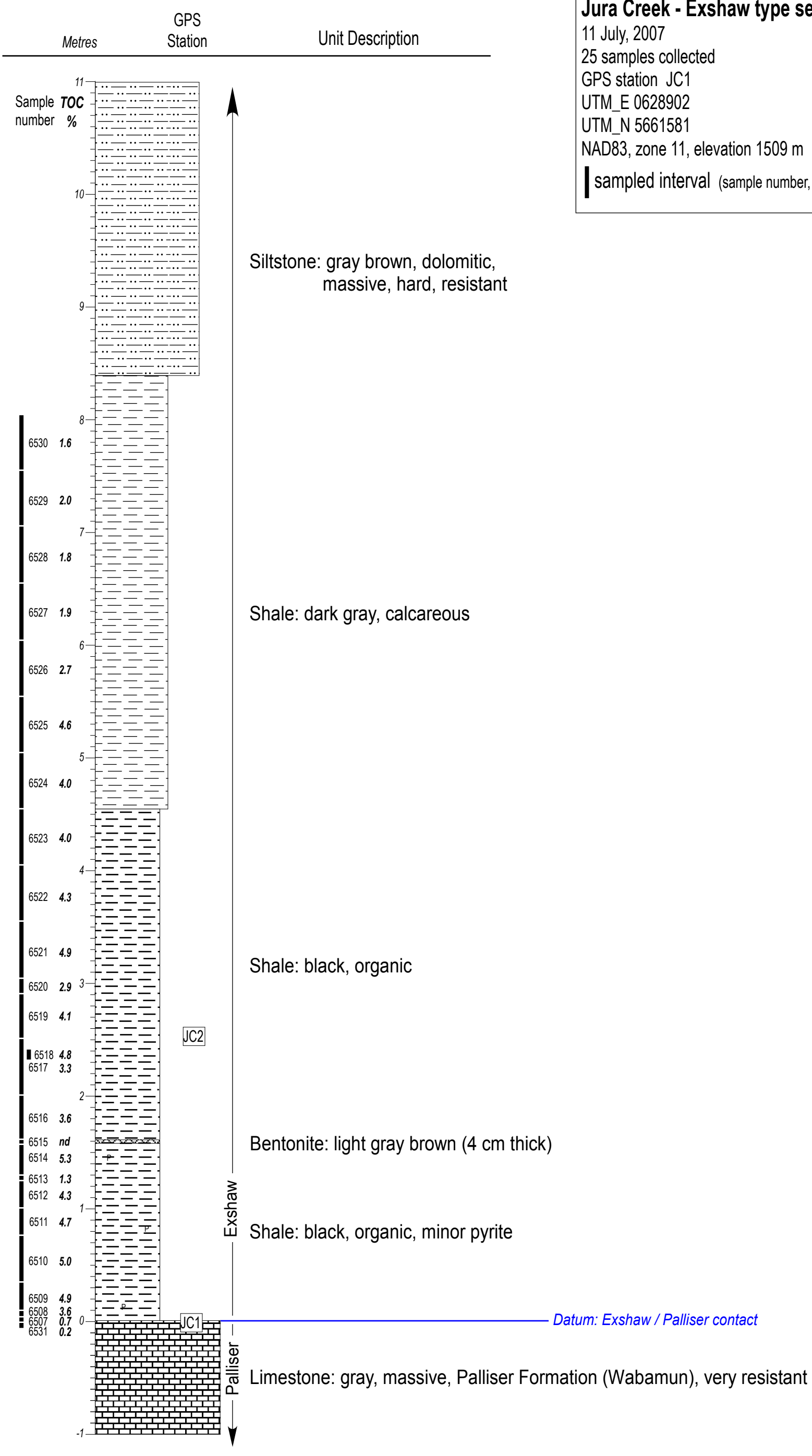

Jura Creek - Exshaw type section

11 July, 2007
25 samples collected
GPS station JC1
UTM_E 0628902
UTM_N 5661581
NAD83, zone 11, elevation 1509 m

| sampled interval (sample number, TOC %)

Nordegg Banff Section

Sample Number	TOC %	Metres	GPS Station	Unit Description
				Covered
7313	0.2	120m	N04	Lime mudstone: dark gray, massive, resistant
		110		
7312	0.2			
7311	0.3	100		
		90		
7310	0.2			Interbedded Lime mudstone and Shale: Ls: dark gray, 10 to 20 cm beds interbedded with 1-3 cm very dark gray shale, This unit is mostly covered with surface vegetation and soil.
7309	0.3	80		
7308	0.5			
7307	0.3	70		
7305	0.3			
7304	0.3	60		
7303	0.3			
7302	0.4	50	N03	
7301	0.3			
		40		Lime mudstone: dark gray, thick bedded to massive, strongly calcareous, resistant, minor silt-stone laminae and chert, beds are thickening upward
6550	0.4			
		30		
6549	0.2			
6548	0.3	20		Lime mudstone: dark gray, finely bedded (5 to 10 cm), strongly calcareous, light gray brown silt-stone beds and lenses, black chert nodules and beds, hard, resistant
6547	0.3			
6546	0.5		N02	Shale: black, dark brown weathering, soft, recessive
6545	0.3	10		Siltstone/shale: dark gray brown, silty, calcare-ous, 2 to 5 cm beds with thin shale interbeds, resistant
6533	1.1			Shale: black, soft, platey, recessive
6543	0.7			
6542	0.9			Mudstone/siltstone: light gray brown, dolomit-ic, very slightly calcareous, massive, resistant
6541	0.3			
6540	0.2			
6539	4.2			Shale: black, organic, soft, recessive 2 cm ben-tonite bed .5m from top
6534	2.3			
6538	3.0	0	N01	
6537	2.8			
6536	0.1			Limestone: gray, massive, Palliser Formation (Wabamun), very resistant, exposed for > 50m
		-10		

Banff

Exshaw

Palliser

Datum: Exshaw / Palliser contact

Nordegg railway section
22 August, 2007
29 samples collected
GPS station N01
UTM_E 0567642
UTM_N 5816426
NAD83, zone 11, elevation 1327 m

6534 *2.3* sample point, sample #, TOC %

Appendix 3 – Well Logs, Core and Type of Analysis Run on Each Sample

15-03-10-10W4_top

15-03-10-10W4_bottom

12-36-30-22W4

08-27-39-11W5

09-06-52-11W5

07-08-74-14W5

06-02-79-22W5

15-27-98-25W5

04-23-72-10W6

08-08-76-07W6

16-24-77-6W6

02-14-82-02W6

08-30-82-02W6

06-04-84-07W6

15-05-107-08W6

00/15-03-010-10W4/0

KB 869.0 m

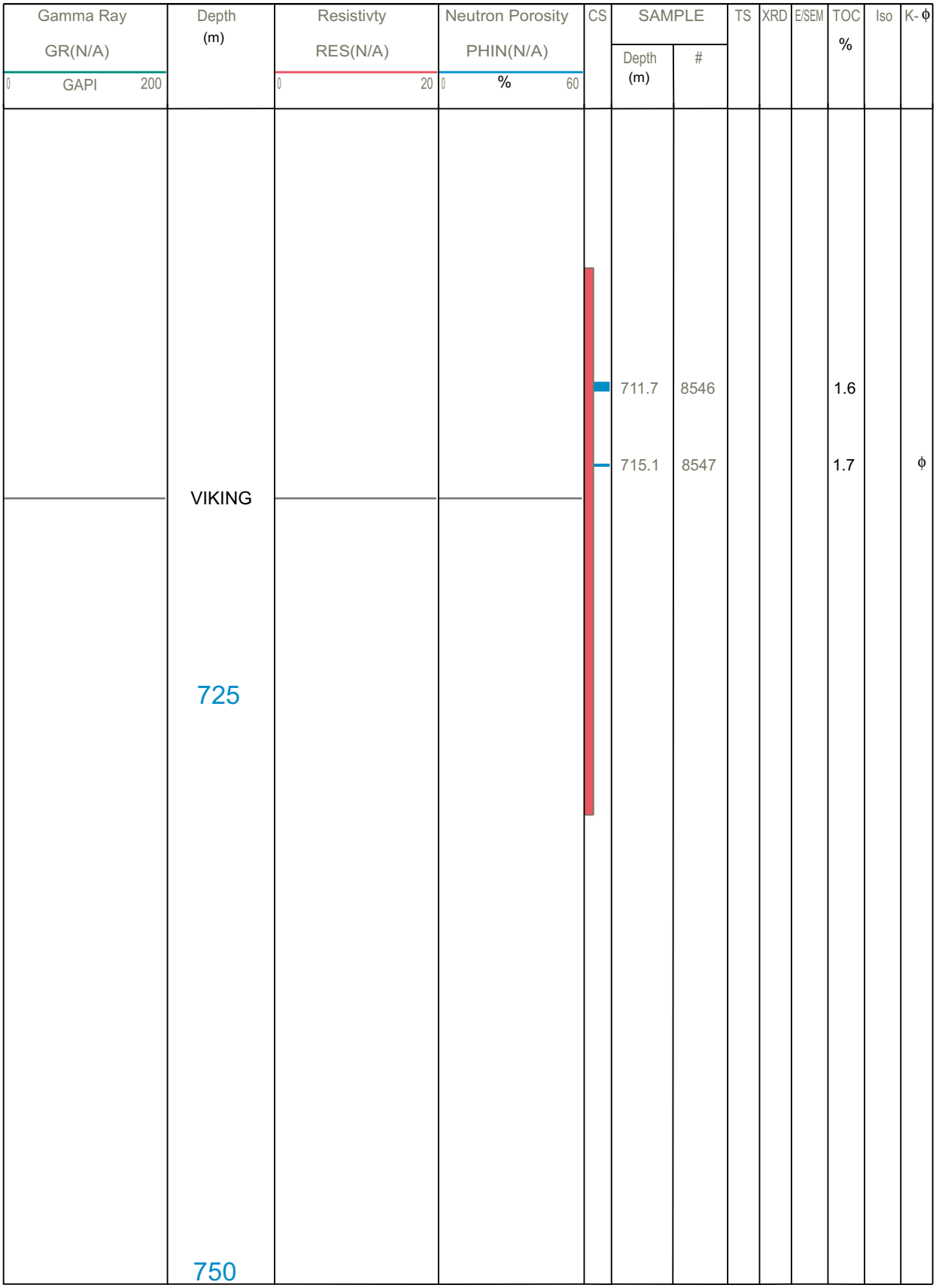

00/15-03-010-10W4/0

KB 869.0 m

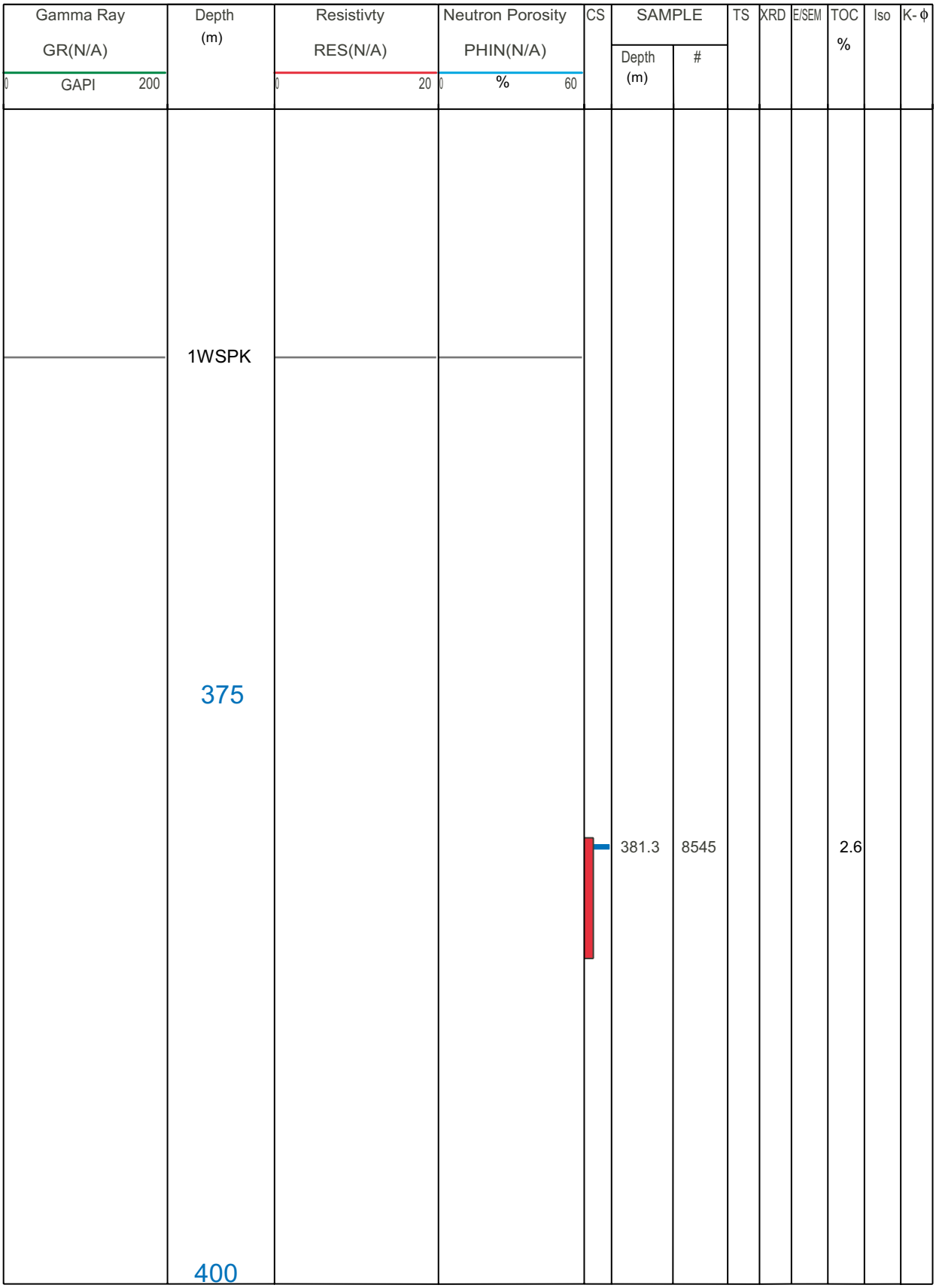

00/12-36-030-22W4/0
KB 840.3 m

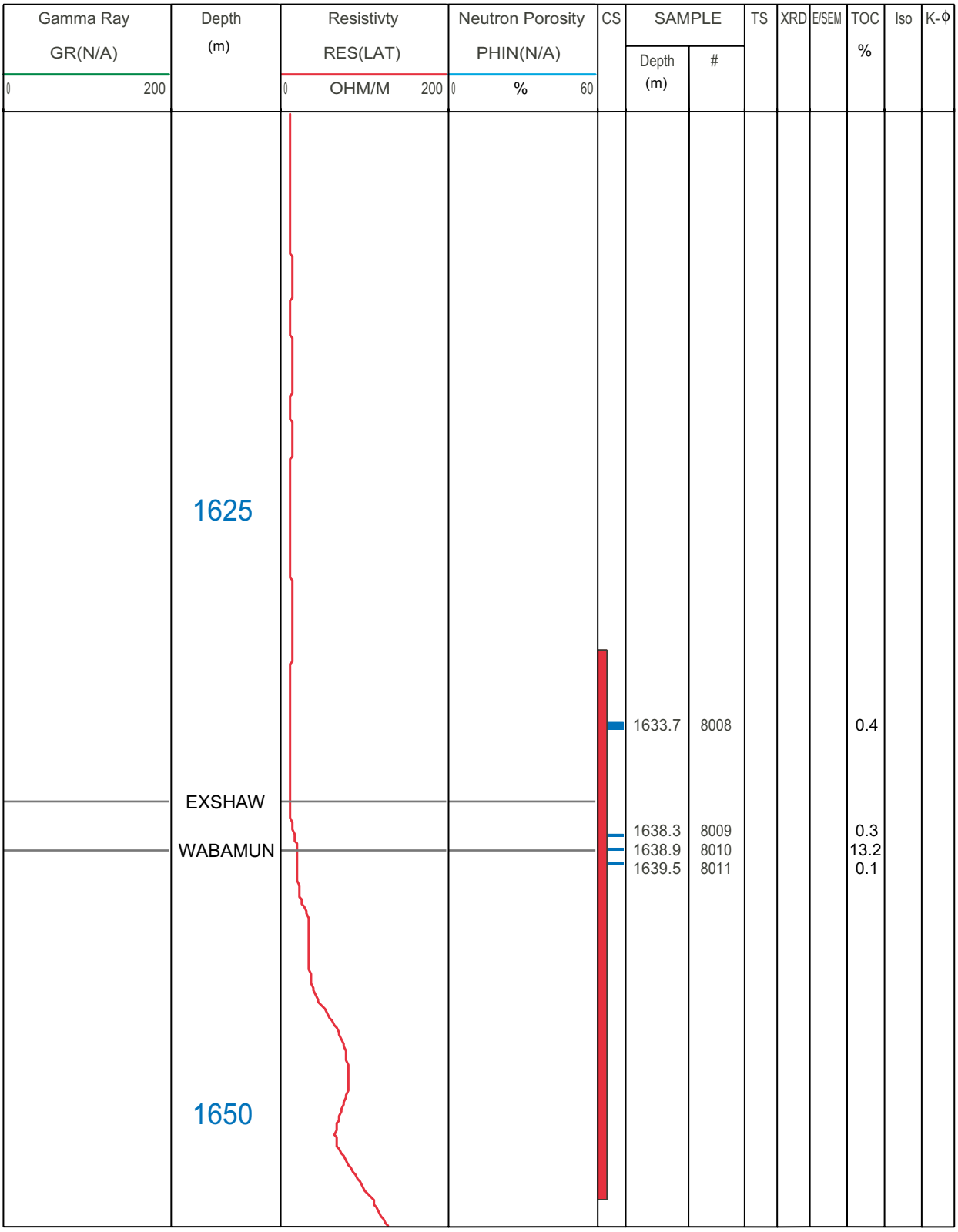

00/08-27-039-11W5/0
KB 1168.6 m

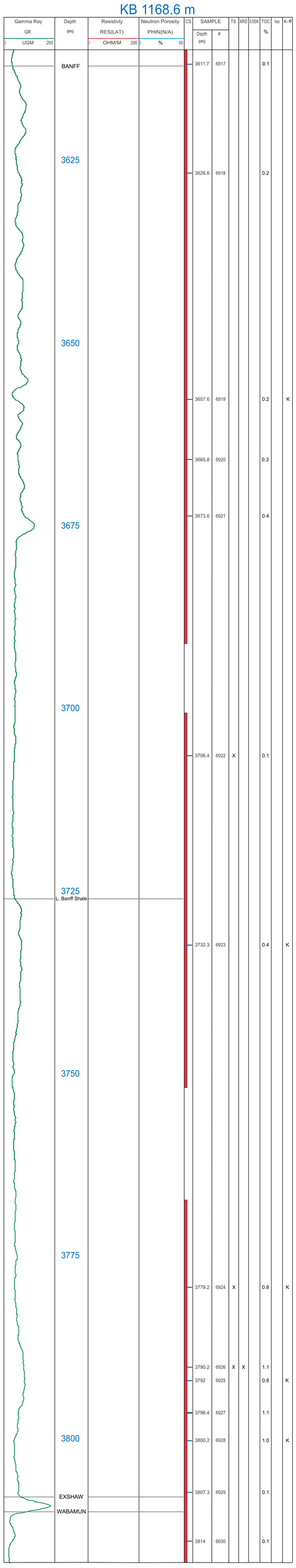

00/09-06-052-11W5/0
KB 940.6 m

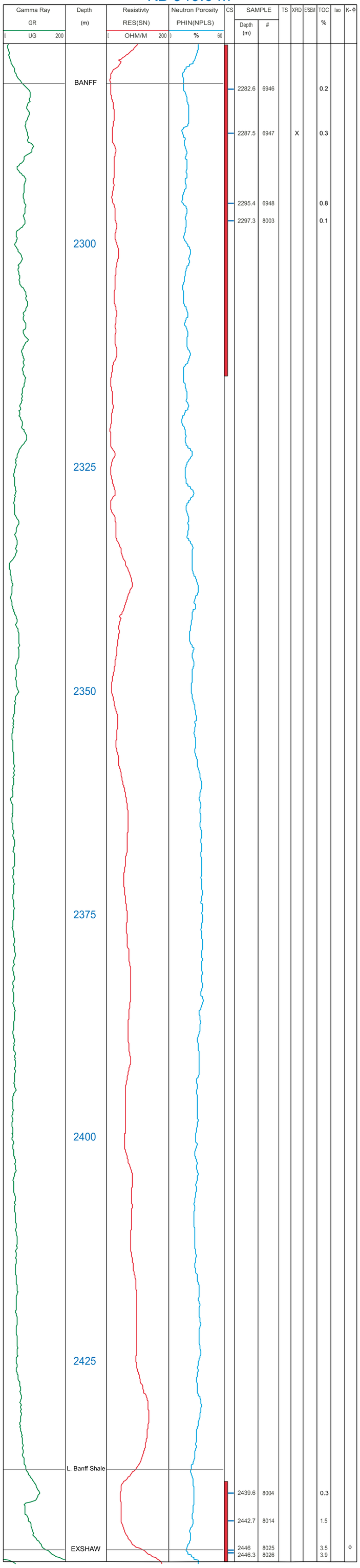

00/07-08-074-14W5/0
KB 592.8 m

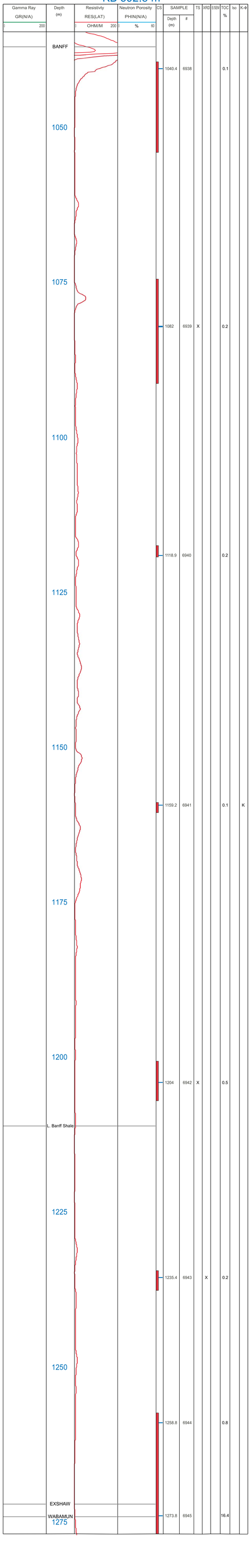

00/06-02-079-22W5/0
KB 581.6 m

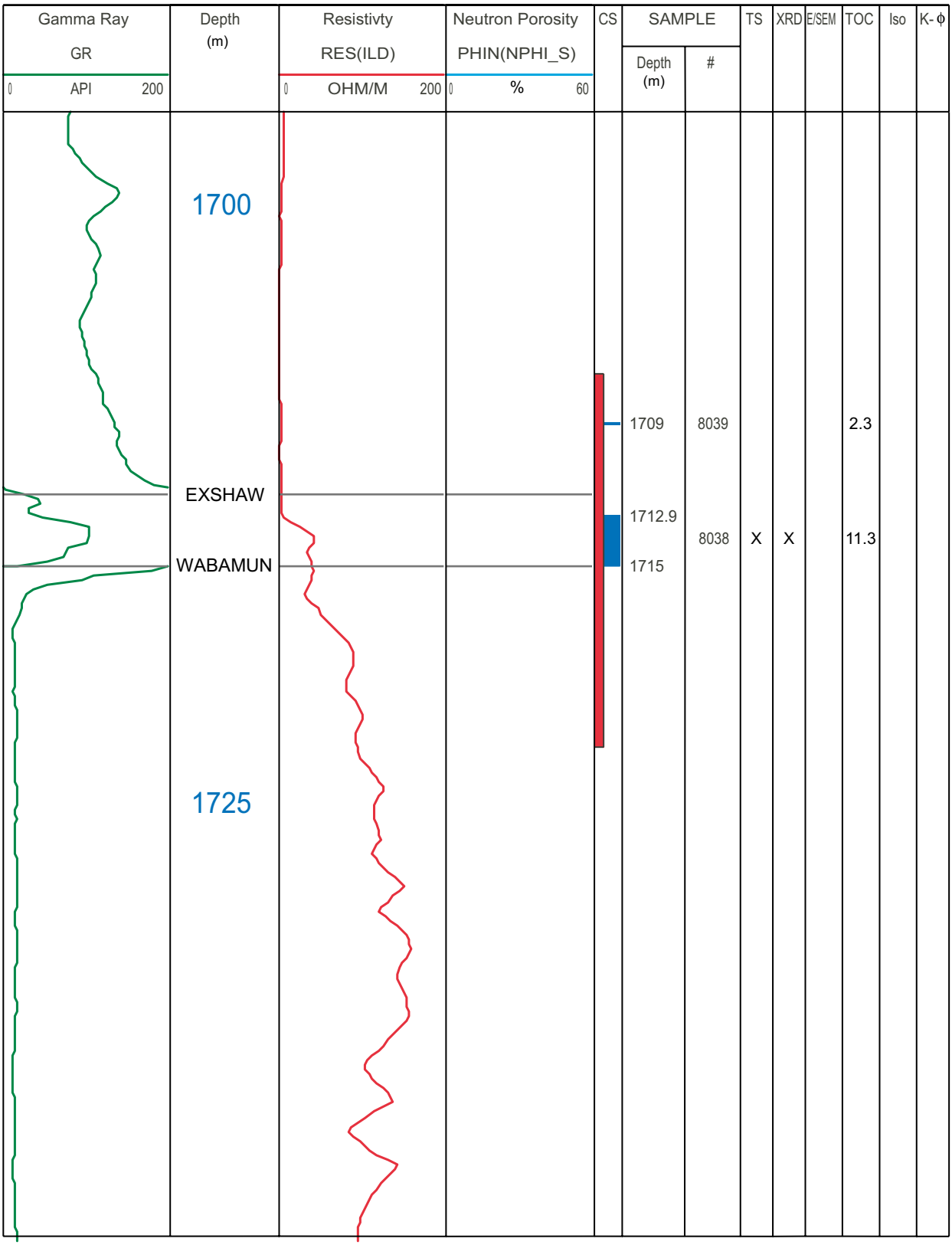

00/15-27-098-25W5/0

KB 892.2 m

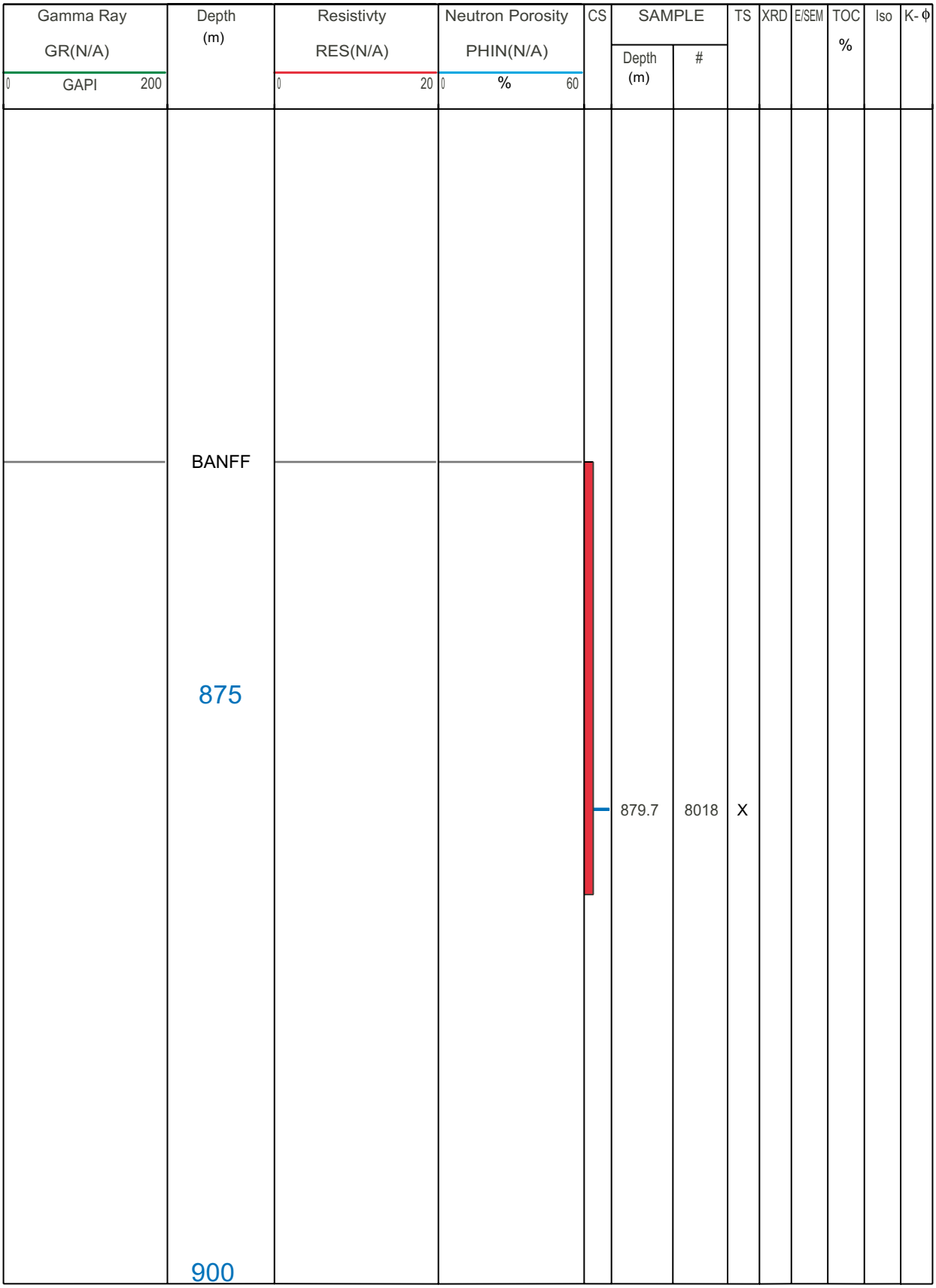

00/04-23-072-10W6/0

KB 776.3 m

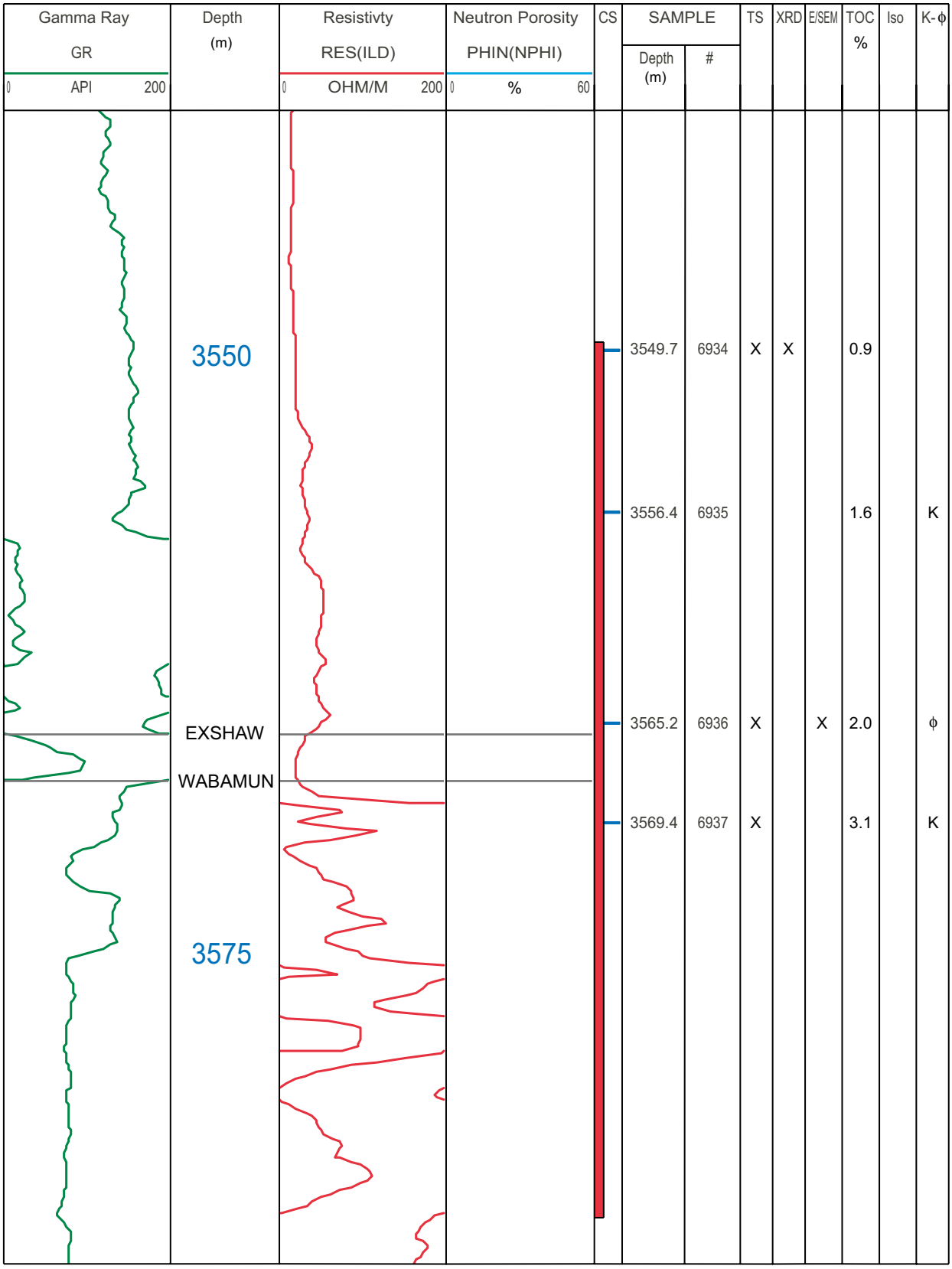

00/08-08-076-07W6/0
KB 779.2 m

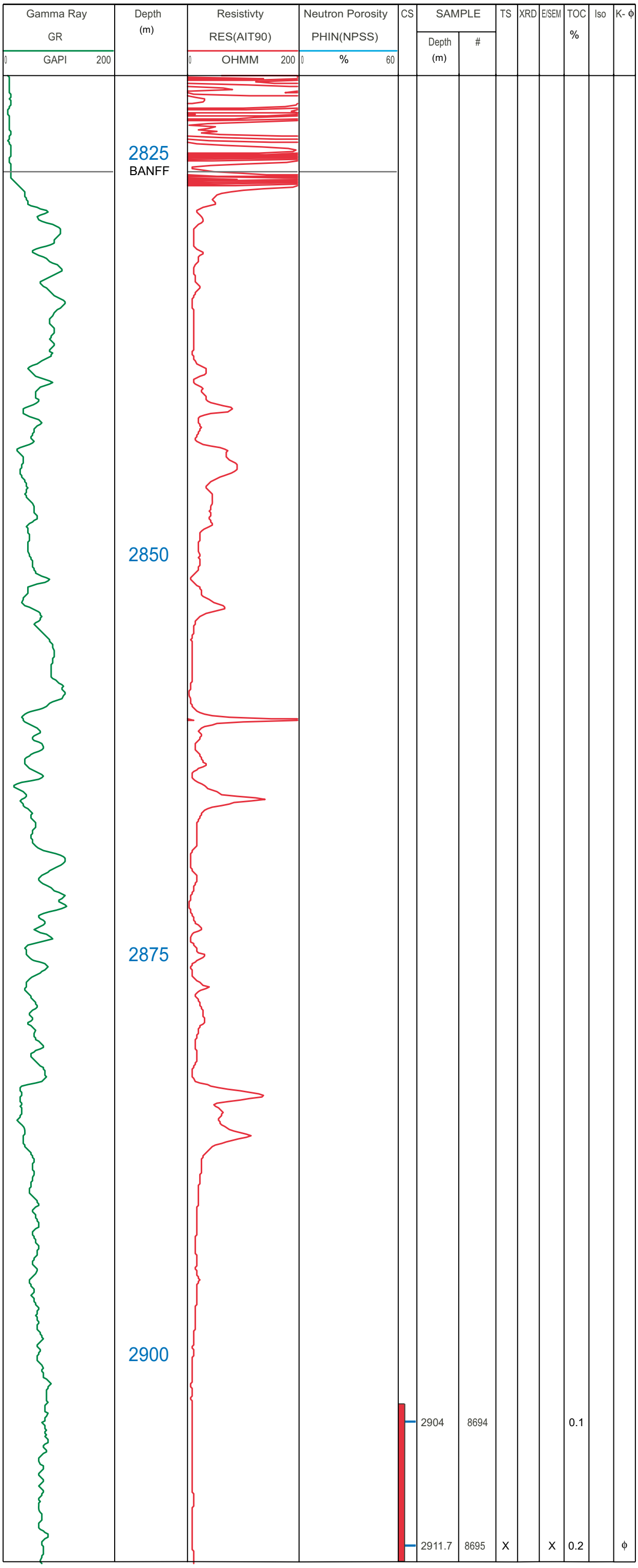

00/16-24-077-06W6/0
KB 646.0 m

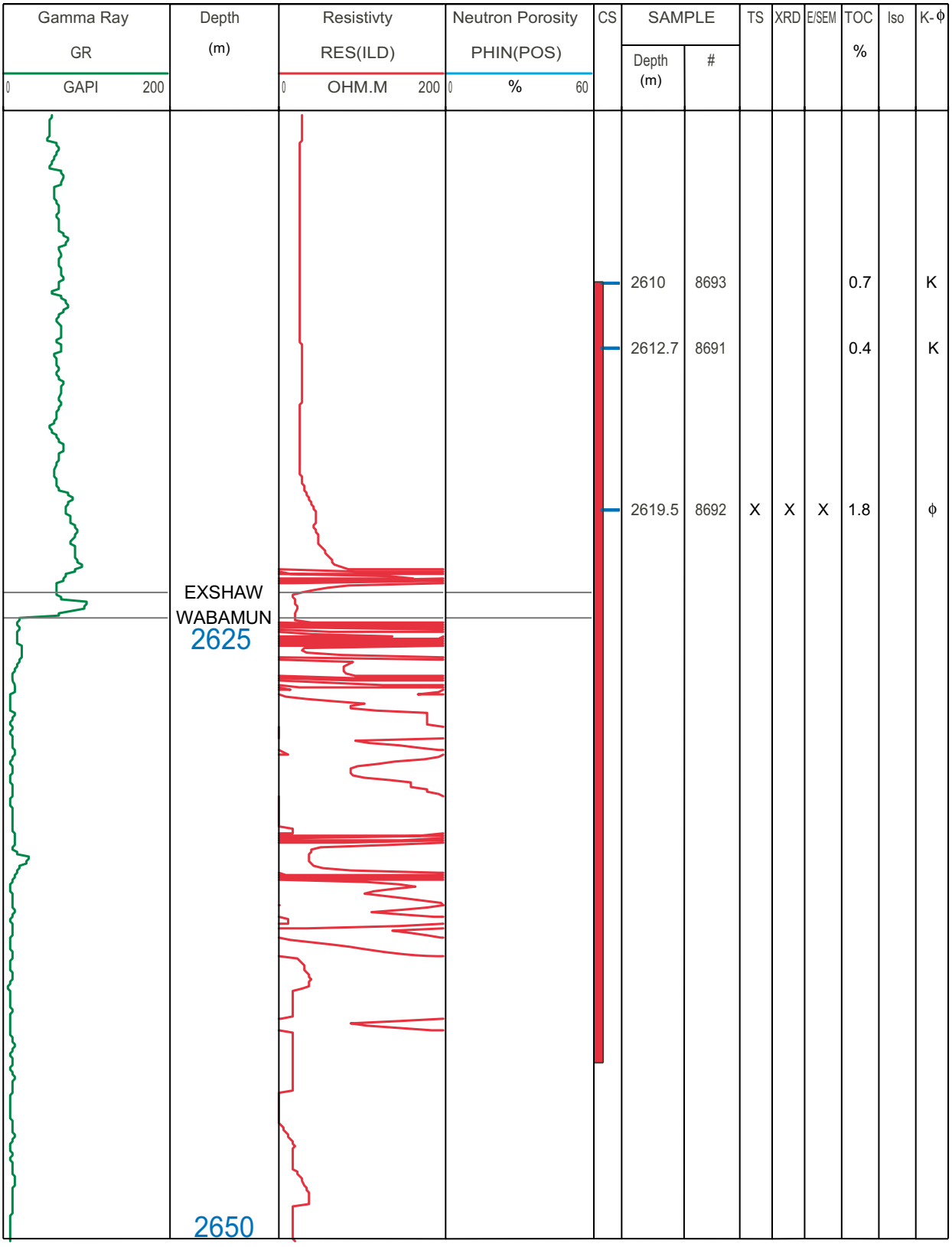

00/02-14-082-02W6/0

KB 666.9 m

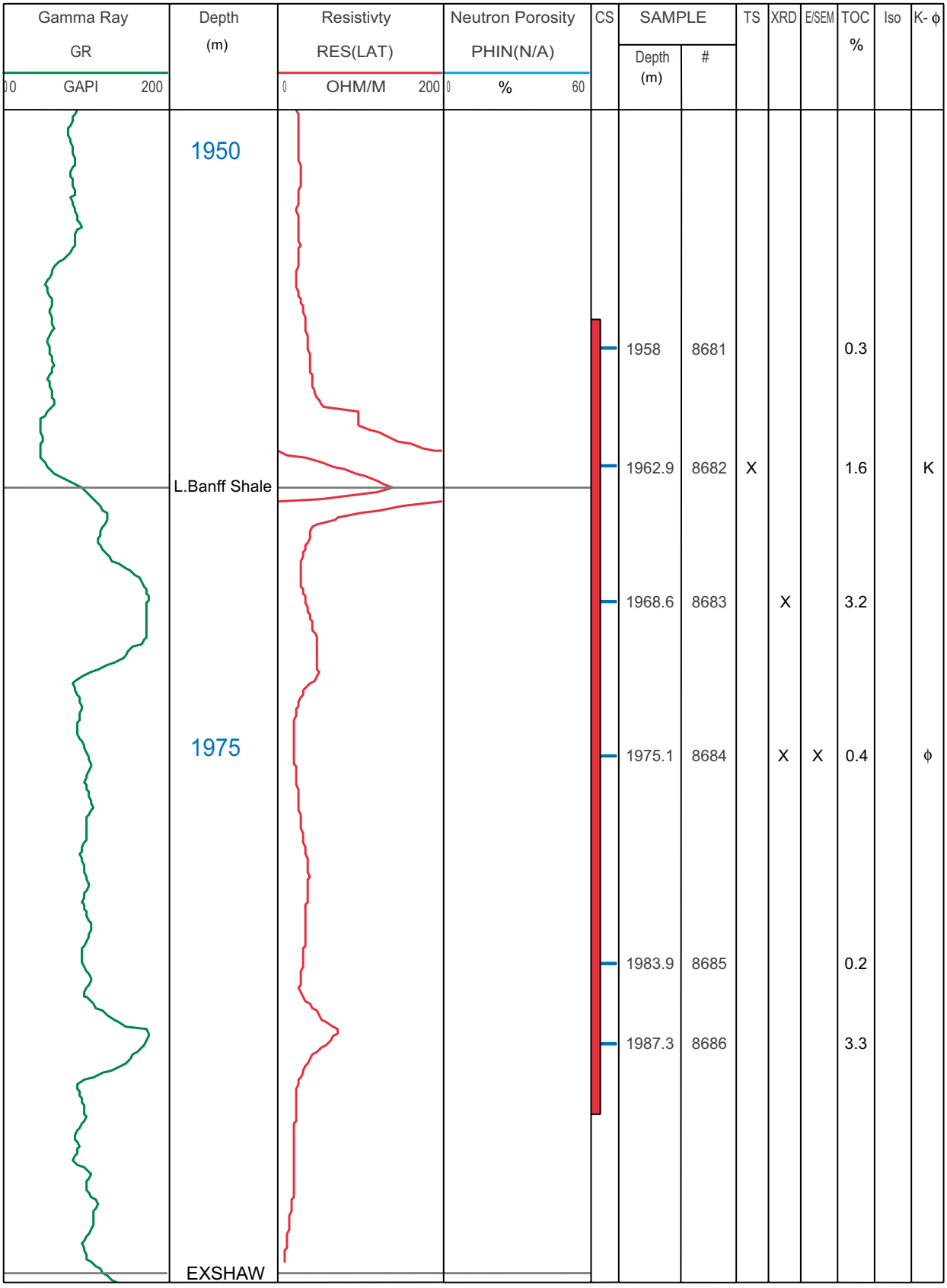

00/08-30-082-02W6/0
KB 705.2 m

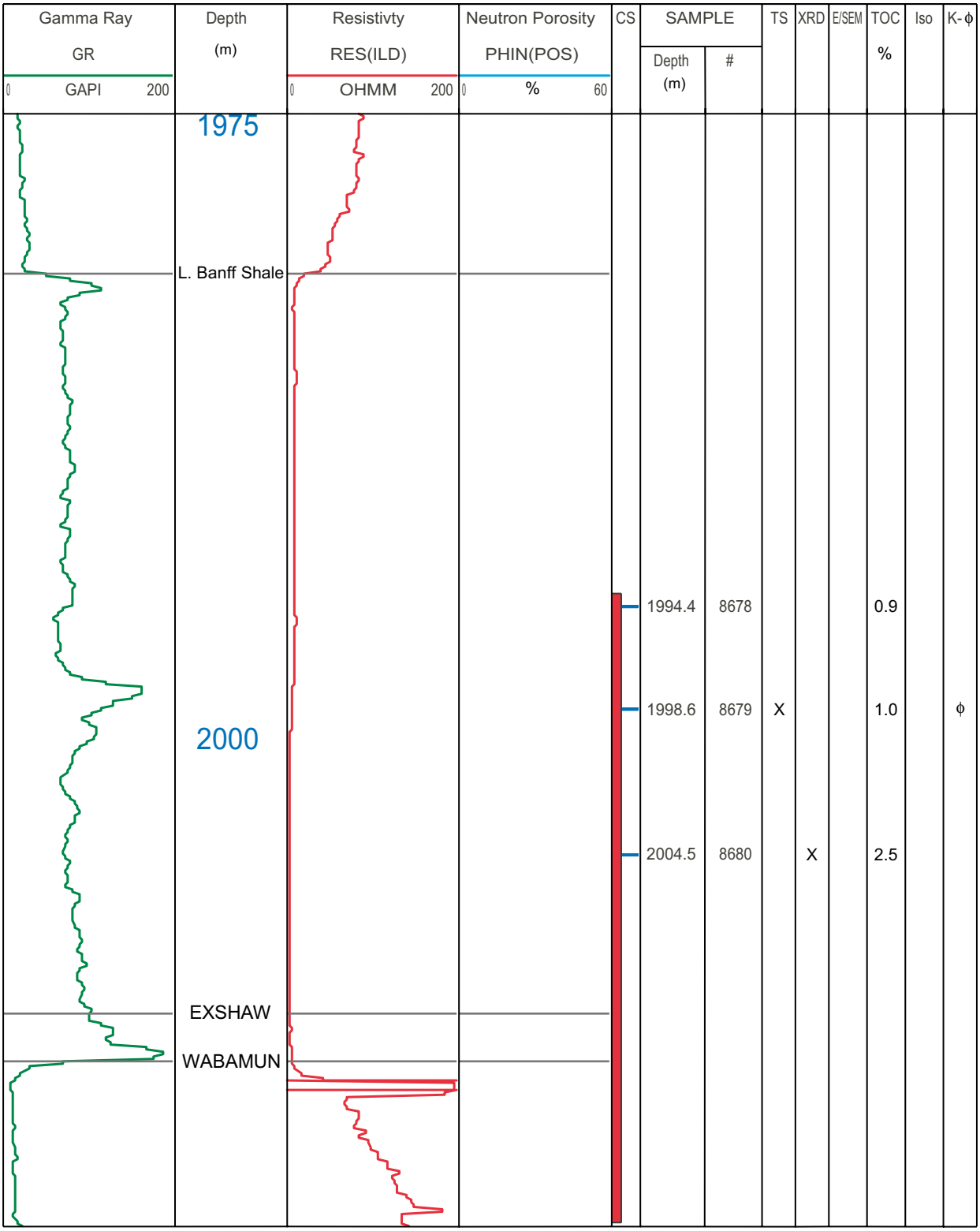

00/06-04-084-07W6/0
KB 670.3 m

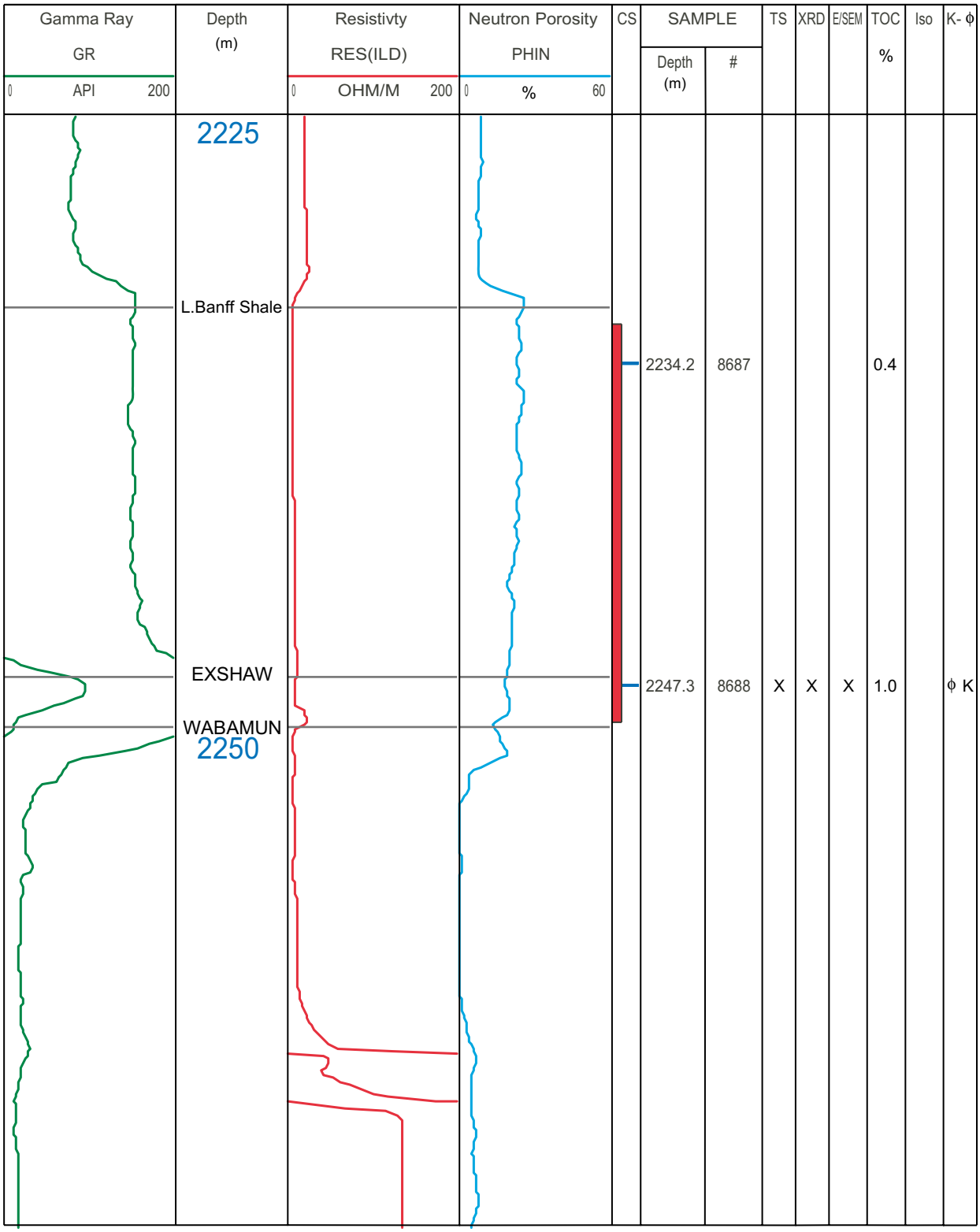

00/15-05-107-08W6/0
KB 531.3 m